Quality markers screening of traditional Chinese medicine prescriptions based on the multi-factor analysis strategy: Jin-Zhen oral liquid as a case

Ling-xian Liu [a,1], Hai-bo Li [b,1], Jia-ying Zhang [a], Dan-feng Shi [a], Zhen-zhong Wang [b], Xin-sheng Yao [a,*], Wei Xiao [b,*], Yang Yu [a,*]

[a] Institute of Traditional Chinese Medicine & Natural Products, College of Pharmacy and State Key Laboratory of Bioactive Molecules and Druggability Assessment, Jinan University, Jinan University, Guangzhou 510632, China
[b] National Key Laboratory on Technologies for Chinese Medicine Pharmaceutical Process Control and Intelligent Manufacture and Jiangsu Kanion Pharmaceutical Co. Ltd., Jiangsu, Lianyungang 222001, China

A R T I C L E   I N F O

A B S T R A C T

Background: Jin-Zhen oral liquid (JZOL), a well-known traditional Chinese medicine prescription (TCMp), has extensively been used to treat acute bronchitis in children more than four hundred years in China. However, the current quality control standard of JZOL is inadequate, posing challenges for its internationalization.
Purpose: In this study, a Q-marker screening strategy based on multi-factor analysis was proposed to comprehensively evaluate anti-inflammatory Q-markers of Jin-Zhen oral liquid (JZOL).
Methods: Firstly, the chemical profile and the pharmacokinetics properties of multiple components in JZOL were characterized by UPLC-Q/TOF-MS and UPLC-QqQ-MS. By integrating the measurable and absorbed components, twenty-two components with structures accurately defined, were selected as candidate Q-markers of JZOL. Following that, a network connecting 22 components and targets closely associated with bronchitis was established. Afterwards, a multi-factor analysis mode was developed to balance the components' multiple characteristics, and screen out the anti-inflammatory Q-markers in JZOL. Finally, the anti-inflammatory activity evaluation was conducted by LPS-induced RAW 264.7 macrophages to prove the representativeness of anti-inflammatory Q-markers in JZOL.
Results: As a result, a total of 92 components were characterized in JZOL and the pharmacokinetics properties of 11 bioactive components *in vivo* were further characterized. Then, an overlapping of 46 targets involved in the interactions of selected 22 candidate Q-markers and the regulation of bronchitis inflammation were collected. Subsequently, a multi-factor analysis was developed on 22 candidate anti-inflammatory Q-markers covering five factors, with the statistic KMO values of 0.645, and the P values of Bartlett's Test equal to 0.000. A total of seven ingredients (aloeemodin-8-O-β-D-glucopyranoside, baicalin, chrysin-7-O-β-D-glucuronide, oroxylin A 7-O-β-D-glucuronide, wogonoside, chrysophanol-8-O-β-D-glucopyranoside, and skullcapflavone II) were selected as Q-markers of JZOL, and the inhibitory effects of these candidate Q-markers on the secretion of inflammatory cytokes (NO, IL-6, IL-1β, and PGE$_2$) in lipopolysaccharide (LPS)-stimulated RAW264.7 cells were evaluated and confirmed.
Conclusion: This study not only offers a fresh approach to uncovering Q-markers in the quality control research of TCMps but also identifies the suitable anti-inflammatory Q-markers for JZOL for the first time, with the potential to serve as a reference for existing quality control standards of JZOL.

1. Introduction

Traditional Chinese Medicine prescriptions (TCMps) with the characteristics of "multi-components, multi-targets, and multi-pathways" have been used to treat a variety of ailments for thousands of years (Kurniawan, Y.S., 2023; Chu et al., 2022). Quality control of TCMps is not only essential for their clinical efficacy and safety but also plays a significant role in their internationalization and modernization process (Ouyang et al., 2022; Wang et al., 2016). However, the quality of TCMps is frequently inconsistent due to various factors such as variety, origin, processing method, and the interaction of components derived from different herbs, posing a significant challenge for dependable quality control of TCMps. To address this issue, a novel concept of quality marker (Q-marker) has been proposed recently to improve the consistency of TCMps' quality (Liu et al., 2017; Liu et al., 2016).

Q-markers are the efficacy-related essential components naturally existing in individual herbs that can be determined qualitatively and quantitatively, and closely linked to the compatibility theories of Traditional Chinese Medicine. Ideal TCMp Q-markers should possess properties including traceability, specificity, bioactivity, measurability, and compatibility contribution (Liu et al., 2021). However, screening for suitable Q-markers from hundreds and thousands of ingredients in TCMps is a significant challenge. To reveal Q-markers in TCMps, several methods have been developed, such as the metabolomics (Gao et al., 2022), chinmedomics approach (Xiong et al., 2020), network pharmacology (Liu et al., 2020), pharmacokinetic analysis (He et al., 2018), and systems biology (Li et al., 2022). Nevertheless, conventional approaches are inadequate in providing a comprehensive and intuitive assessment of the various characteristics of Q-markers. Therefore, balancing various properties and screening out pivotal Q-markers of TCMps remains a challenge and requires a comprehensive evaluation strategy.

Jin-Zhen oral liquid (JZOL) is a famous prescribed TCMps comprising eight medicines: Caprae Hircus Cornu, Scutellariae Radix, Fritillariae Ussuriensis Bulbus, Rhei Radix et Rhizoma, Gypsum Fibrosum, Bovis Calculus Artifactus, Chloriti Lapis, and Glycyrrhizae Radix et Rhizoma. Double-blind, placebo-controlled clinical trials with centralized, randomized controlled studies (Liu et al., 2014; Lu et al., 2010) have confirmed its clinical efficacy in treating acute bronchitis (Shu et al., 2018; Sun et al., 2016; Zhang & Gu, 2016), and it may exert anti-inflammatory effects by regulating the TLR4/MyD88/NF-κB signaling pathway (Li et al., 2023). The pharmacological activity may attribute to its composed medicinal herbs, including Scutellariae Radix (Zhu et al., 2023), and Rhei Radix et Rhizoma (Hu et al., 2021) which possess significant anti-inflammatory properties in various diseases. JOZL has been found to have a broad-spectrum anti-inflammatory in clinical practice, primarily utilized for treating various respiratory conditions in children (Cui et al., 2022, Yang, 2021). Accordingly, the current quality evaluation marker (The Pharmacopoea Commission of PRC, 2020) is inadequate in representing the overall efficacy of JZOL, as it fails to reflect the combined anti-inflammatory effects through multiple components present in TCMps.

In this study, an anti-inflammatory Q-marker screening strategy based on multiple factors analysis was first proposed and applied to a research example of JZOL (Fig. 1). Based on the scientific concept of Q-marker, the quality control index of JZOL should fulfill the requirements in terms of specificity, quality transferability, measurability, compatibility, and pharmacological efficacy. Therefore, we first characterized the chemical profile of JZOL using UPLC-Q/TOF-MS to ensure chemical specificity and measurability. Secondly, the pharmacokinetic (PK) properties were investigated to follow the requirement of feature transferability from in vitro to *in vivo*. Thirdly, the pharmacological efficacy was primarily considered based on the components and related targets. Inspired by the previous work on content analysis (Li et al., 2020a) and metabolic analysis (Zhang et al., 2020), a multi-factor mode was developed to screen out JZOL Q-markers that balanced multiple characteristics (the compatibility contribution of herbal medicines, the content, the *in vivo* PK characteristics, and the degree of network pharmacology). Afterwards, the mentioned factors were normalized and subjected to multi-factor analysis, with the suitability for analysis being evaluated through pre-calculation and applicability testing, and the Q-Markers was chosen based on the ranking of the F value. Finally, the activity evaluation was conducted to verify the feasibility of Q-markers
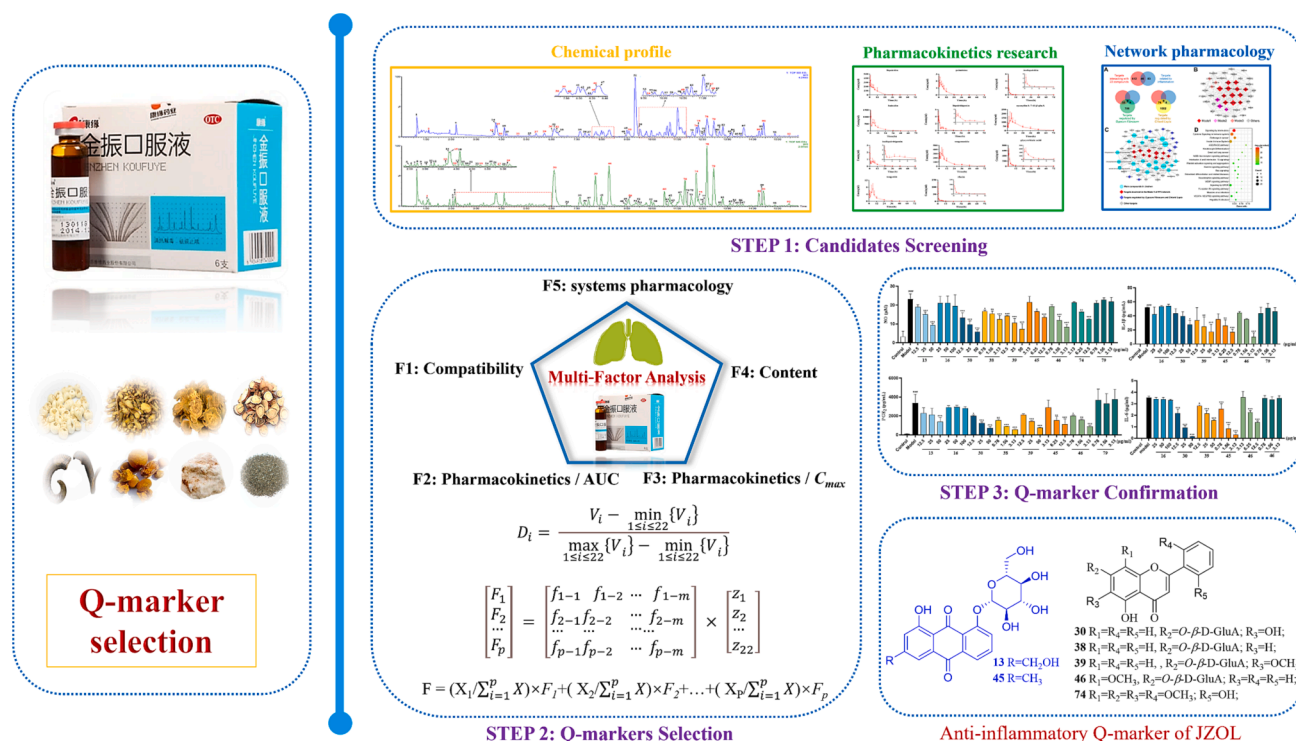
Fig. 1. The novel strategy for the discovery of Q-markers in JZOL based on "multi-factor analysis".

in JZOL. In a summary, this study presents a fresh approach for disclosing Q-markers in TCMps and helps to find superior Q-markers of JZOL to improve its quality control measures.

2. Experiment and methods

2.1. Materials and chemicals

Liquiritigenin apioside and licorice-saponin G2 were isolated in our laboratory, and their structures were unambiguously identified by nuclear magnetic resonance (NMR) and MS methods. The other reference standards were purchased from National Institutes for Food and Drug Control., Chengdu Puruifa Medical Technological Co., Ltd (Chengdu, China), Lemeitian Co. Ltd (Chengdu, China), Shanghai yuanye Bio-Technology Co., Ltd (Shanghai, China) and Shanghai Macklin Biochemical Co., Ltd (Shanghai, China). Detailed information regarding the reference standards used in this study is presented in Table S1.

JZOL was provided by Jiangsu Kanion Pharmaceutical Co. Ltd. (No. 181026, Lianyungang, China). Scutellariae Radix, Fritillariae Ussuriensis Bulbus, Rhei Radix et Rhizoma, Bovis Calculus Artifactus, and Glycyrrhizae Radix et Rhizomawere were purchased from the Ji'an Medical Material Market (Jiangxi, China). All herbal medicines were identified by Prof. GuangXiong Zhou of Jinan University, and voucher specimens were deposited at Institute of Traditional Chinese Medicine & Natural Products, college of pharmacy, Jinan, University, Guangzhou, China.

LC-MS grade acetonitrile: Fisher Scientific, LC-MS-grade formic acid: Sigma-Aldrich, Water: Watsons. Methanol, and ethanol used for sample extraction were of analytical grade. Details of other materials are recorded in the corresponding methods.

2.2. Sample preparation

JZOL was directly evaporated with a rotary evaporator and then diluted to a concentration of 10 mg/mL. Subsequently, 2 mL of these solutions were transferred into a separate clean tube, dried under a nitrogen gas stream at room temperature, and then suspended in 2 mL of water. For the Solid-phase extraction (SPE, Vac 3 cc, 200 mg Phenomenex strata C18-E cartridges from Torrance, CA) process: the cartridge were pre-conditioned with 3 mL of methanol, followed by 3 mL of water before application. The centrifuged supernatants were loaded onto the SPE cartridges and washed with 2 mL of water. Afterward, an elution step was performed using 4 mL of methanol, and the eluted solution was collected. Supernatant aliquots of 2 μL centrifuged supernatant were then injected into the LC-MS system.

2.3. Animals and drug administration

Healthy male Sprague Dawley rats, weighing 200 ± 20 g, were purchased from the experimental animal center of Guangdong province (Guangzhou, China). All animals were randomly assigned to groups and maintained under standard condition (23 ± 2 °C and 55–60 % relative humidity). The rats were given free access to water and standard chow for a week before the experiment. Next, the drug-treated group (n = 7) was administered JZOL at the dose of 3.31 g/kg/day (equal clinical dose). Blood samples (0.3 mL) were collected from the jugular vein and placed in heparinized tubes at 0.25, 0.5, 1.0, 2.0, 4.0, 6.0, 8.0, 12.0, 24.0, 36.0, 48.0 and 72.0 h after the drug administration. After centrifuging (14,000 rpm, 4 °C) the blood sample for 10 min, the obtained plasma was stored at −80 °C.

2.4. Pretreatment of biological samples

A volum of 100 μL plasma sample was spiked with 50 μL of IS and 400 μL of 0.5 % formic acid in acetonitrile for protein precipitation. Following a 2-minute vortexing and subsequent centrifugation (14,000 rpm, 20 min), the supernatants were dried to completion using nitroge. The residue was reconstituted in 100 μL methanol and vortexed for 2 min. After centrifuged (14,000 rpm, 20 min), an aliquot of 2 μL was injected into the LC-MS system for analysis.

2.5. UPLC-Q/TOF-MS analysis

UPLC analyses: ACQUITY™ UPLC I-Class system, binary solvent system, and an automatic sample manager. Q/TOF-MS analyses: Waters SYNAPT™ G2 mass spectrometer (Waters, Manchester, UK), and an ESI interface. The detail information of optimal conditions was presented in **supplementary material**.

2.6. UPLC-QqQ-MS analysis

Components were detected under a Xevo TQ-XS mass spectrometer (Waters Corp., Milford, MA, USA) equipped with electrospray ionization (ESI) interface. Detailed information regarding the optimal conditions can be found in the **supplementary materials**. The most appropriate precursor ion, daughter ion, cone voltage, and collision energy were optimized and displayed in **Table S2**.

All experimental data were collected and processed by Waters Masslynx™ software 4.1 and the Quanlynx program (Waters, Milford, MA, USA).

2.7. Method validation of pharmacokinetic research

The method validation was carried out according to the 2018 Food and Drug Administration (FDA) guidelines on bioanalytical method validation in terms of selectivity, linearity, accuracy, matrix effect, precision, and stability. The detail information of method validation was presented in **supplementary material**.

2.8. The candidate Q-markers selection

Twenty-two components, whose structures are all well-defined by the reference standards, covering the characteristics of multiple structural types (flavonoids, triterpenoid saponins, alkaloids, bile acids, anthraquinones and others), higher content (11.56 ~ 867.40 μg/mL), and bioavailable constituents *in vivo* (absorbed in blood) were selected as candidate Q-markers of JZOL based on the researches of qualitative and quantitative chemical analysis, as well as PK study. In detail, the selection of the 22 components was a comprehensive compilation, consisting of 13 components that could be measured for in vitro content, and 21 prototypes (Table S3, Fig. S1) (Table S3, Fig. S1) that were accurately identified with reference standard for *in vivo* verification.

2.9. Network pharmacology studies

The structures of selected candidate Q-markers in JZOL were prepared in SMILES format, and imported into the SwissTargetPrediction (https://www.swisstargetprediction.ch/) for the prediction of targets in "homo sapiens" species (Gfeller et al., 2014). The target set was created to explore potential interactions between protein targets and the compounds in JZOL. As the Drugbank database (https://www.drugbank. ca/) provides comprehensive profiles of protein targets associated with clinical symptoms (Wishart et al., 2018), the protein targets involved in the symptom of "inflammation" were systematically searched and derived as a target set of inflammation. The target sets involved in the regulation of Gypsum Fibrosum and Chloriti Lapis was respectively derived from the STITCH server (https://stitch.embl.de/) (Kuhn et al., 2014) based on the main ionic components including Ca^{2+}, $SO4^{2-}$, Fe^{2+}, Mg^{2+}, K^+, Na^+ (Ikarashi et al., 2012; Chen et al., 2022). These target sets were compared and overlapped to get the common targets for further analysis (Amala et al., 2023).

The key targets involved in the interactions of 22 compounds and the

symptom of "inflammation" were collected for bioinformatics analysis. The Search Tool for the Retrieval of Interacting Genes (STRING) database (https://string-db.org/) is used to input all essential targets for protein–protein interaction (PPI) prediction (Szklarczyk et al., 2021). The detail information was supported in **supporting information**. The regulation effect of 22 compounds of JZOL as well as the main ionic components of Gypsum Fibrosum and Chloriti Lapis were characterized by their involved key targets, while the corresponding signaling pathways were further analyzed by gene set enrichment analysis (GSEA) (version 3.0, https://software.broadinstitute.org/gsea/). The top 20 items with the most significant were derived for further analysis.

The importance of targets that involved in the interactions of 22 compounds and the symptom of "inflammation" were further evaluated by molecular docking using Glide 6.6 of Schrödinger Software Suite (Schrödinger, LLC, New York, NY, 2015). The 3D crystal structures for 46 unique targets were retrieved from the Protein Data Bank database (https://www.rcsb.org/) or the AlphaFold protein structure database (https://alphafold.ebi.ac.uk/). The target structures were initially readied by introducing hydrogen atoms, rectifying absent side chains, and conducting minimization using the Protein Preparation Wizard module. Thereafter, the binding pocket for each target was defined according to the location of the co-crystalized ligand or the best site predicted by the fpocket software.

The 3D structures of 22 compounds were generated and optimized using the LigPrep module, targeting a pH range of 7.0 ± 2.0. The standard precision (SP) protocol was utilized to conduct docking simulations involving 46 targets and 22 compounds. The best docking score for each target-compound couple in the docking runs was selected for analysis, while the docking scores for those with no binding results were set as 0 (**Table S4**). All other parameters were set as default values.

2.10. Development of multi-factor analysis to balance and screen Q-markers with the multiple characteristics in JZOL

A multi-factor analysis mode was developed to balance the Q-markers related multiple characteristics and to screen the Q-markers in JZOL. The candidate Q-markers with clear herbal origin were defined as king, minister, assistant, and guide based on the chemical profile characterization and TCM compatibility theory. In addition, the network pharmacology was applied to provide a bridge to link the chemical constituents in TCM prescriptions with the corresponding targets to gain comprehensive insight into the therapeutic mechanism of multi-components. Consequently, a multi-factor analysis mode was developed by SPSSPRO (https://www.spsspro.com/mydata/index) platform, and the properties of compatibility contribution (the candidate Q-markers from King, Minister, Assistant, or Guide herb are defined as 4, 3, 2, and 1, respectively), content, pharmacokinetics (C_{max} and $AUC_{0-\infty}$), and network pharmacology (degree value) were converted into five dimensions. However, there may be missing values among multiple dimensions. For example, although some components are highly exposed in TCM prescriptions, they may not be absorbed *in vivo*. Hence, the supplement of the missing value follows these principles: if the candidate Q-marker cannot be absorbed *in vivo*, its value is filled with 0; if the candidate Q-marker is difficult to quantify accurately, its value is filled with the corresponding average; the missing value of content is filled with the minimum value of content. All the data are then standardized as 0–1 points from minimum to maximum according to Eq. (1). The maximum variance method is used to carry out factor rotation. The KMO value (>0.5) and Bartlett's test ($p \leq 0.05$) are applied to judge whether factor analysis is suitable. The number of extracted factors is determined as the main common factor through the gravel map. Based on the determined common factors at all levels, the ingredients' use obtains an eigenvalue matrix, and by calculating the weight of different common factors, the composite score (Eq.2–3) is ultimately calculated for the sample and ranked.

$$D_i = \frac{V_i - \min_{1 \leq i \leq 22}\{V_i\}}{\max_{1 \leq i \leq 22}\{V_i\} - \min_{1 \leq i \leq 22}\{V_i\}} \tag{1}$$

$$\begin{bmatrix} F_1 \\ F_2 \\ \cdots \\ F_p \end{bmatrix} = \begin{bmatrix} f_{1-1} & f_{1-2} & \cdots & f_{1-m} \\ f_{2-1} & f_{2-2} & \cdots & f_{2-m} \\ \cdots & \cdots & \cdots & \cdots \\ f_{p-1} & f_{p-2} & \cdots & f_{p-m} \end{bmatrix} \times \begin{bmatrix} z_1 \\ z_2 \\ \cdots \\ z_{22} \end{bmatrix} \tag{2}$$

$$F = \left(X1/\sum_{i=1}^{p}X\right) \times F1 + \left(X2/\sum_{i=1}^{p}X\right) \times F2 + \cdots + \left(XP/\sum_{i=1}^{p}X\right) \times Fp \tag{3}$$

V is the variable of corresponding characteristic data of candidate JZOL Q-marker; D is the standardized value of variables; F_1-F_P is the score of each common factor, which is used to calculate the overall score of total factors (F); f means factor coefficient, and z is observed variable, which is calculated by a linear combination of several independent factors and a unique variable (Schreiber et al., 2021). X is the weight of different common factors.

2.11. Confirmation of Q-markers based on anti-inflammatory assays

In a humidified environment at 37 °C with 5 % CO2, RAW 264.7 cells were cultured and introduced into DMEM supplemented with 10 % fetal bovine serum (FBS, Gibco, New York, USA). Cell viability was assessed using the [3-(4,5-dimethyl-thiazol-2-yle) 2,5-diphenyltetrazolium bromide] (MTT, Aladdin, Shanghai, China) colorimetric assay. RAW 264.7 cells were incubated for 24 h in 96-well plates at a concentration of 2 × 105 cells per well. Then the components were dissolved in the medium (containing 1 μg/ml LPS) and given to the test wells. The negative control was treated with complete medium (containing 0.1 % DMSO) and the positive control was treated with 1 μg/ml LPS. After 24 h treatment under normal conditions, the supernatant was collected and analyzed by a commercial NO test kit (Nanjing Jiancheng Biological Engineering Research Institute, China). The IL-6, IL-1β, and PGE$_2$ analysis was measured by ELISA kit (IL-6: Multisciences Biotechnology, Zhejiang, China; IL-1β: R&D system, Minneapolis, MN; PGE$_2$: Enzo Life Sciences, Farmingdale, NY) according to the manufacturer's instructions.

Data: Mean ± SD from three independent experiments. Statistical analysis: GraphPad PRISM v7.04, ANOVA followed by Dunnett's post hoc test, P < 0.05 considered significant.

3. Results

3.1. Chemical profile of JZOL by UPLC-Q/TOF-MS analysis

The chemical constituents in JZOL were systematically investigated by searching online databases or Internet search engines (Chemical Abstracts Service (CAS) database, Massbank, Web of Science, and ChemSpider). As a result, a total of 92 compounds, including 37 flavonoids (23 flavones, 4 chalcones, 4 flavanones, 4 isoflavones, and 2 isoflavanones), 14 triterpenoid saponins, 12 alkaloids, 11 bile acids, seven diterpenoids, six anthraquinones, and five other types of compounds were identified or tentatively characterized in JZOL (Table 1; Fig. 2). Out of these, 28 peaks were further confirmed by comparison with reference standards (**Fig. S2**). The base peak intensity (BPI) profiles of JZOL in both negative and positive ion modes are shown in Fig. 3. The origins of the identified compounds were determined by comparing the base peak chromatograms of JZOL with those of individual single herbs (**Fig. S3 and S4**). Fig. 4 illustrates the detailed fragmentation and proposed fragment pathways for representative compounds. Fig. 4 displays the intricate fragmentation patterns and proposed fragment pathways of representative compounds, while additional in-depth information can be found in the **Supporting Information**.

Table 1
Chemical constituents identified in JZOL by UPLC-Q/TOF-MS.

No	t_R	Selected ion	Elemental Composition	Measured mass	Calculated mass	Mass error	Fragmentations (m/z)	Identification or tentative characterization	Type	Source[a]
1	0.63	[M + Na]$^+$	$C_{12}H_{22}O_{11}$	365.1060	365.1060	0.0	707.2219 [2 M + Na]$^+$; 365.1060 [M + Na]$^+$; 203.0529 [M + Na-$C_6H_{10}O_5$]$^+$	sucrose	O	FL
2*	1.10	[M−H]$^-$	$C_7H_6O_5$	169.0136	169.0137	−0.6	169.0136 [M−H]$^-$; 125.0242 [M−H−CO_2]$^-$	gallic acid	O	DH
3	2.07	[M + H]$^+$	$C_{11}H_9NO_2$	188.0713	188.0712	0.5	188.0713 [M + H]$^+$; 170.0604 [M + H-H_2O]$^+$; 146.0606 [M + H-C_2H_2O]$^+$	2-hydroxy-3-naphthamide	O	PBM
4	2.19	[M−H]$^-$	$C_9H_{10}O_3$	165.0554	165.0552	1.2	165.0554 [M−H]$^-$; 121.0654 [M−H−CO_2]$^-$	paeonol	O	GC
5	2.50	[M + H]$^+$	$C_{27}H_{45}NO_6$	480.3326	480.3325	0.2	480.3326 [M + H]$^+$; 462.3099 [M + H-H_2O]$^+$; 444.2100 [M + H-2H_2O]$^+$	pingbeimine B	A	PBM
6	2.54	[M + H]$^+$	$C_{27}H_{45}NO_5$	464.3370	464.3376	−1.3	464.3370 [M + H-H_2O]$^+$; 446.3199 [M + H-H_2O]$^+$; 428.3100 [M + H-2H_2O]$^+$	pingpeimine A	A	PBM
7	2.57	[M−H]$^-$	$C_{21}H_{22}O_9$	417.1183	417.1186	−0.3	417.1183 [M−H]$^-$; 255.0665 [M−H−Glc]$^-$; 135.0080 [$^{1,3}A_0$]$^-$; 119.0503 [$^{1,3}B_0$]$^-$	neoisoliquiritin	F	GC
8	2.65	[M + H]$^+$	$C_{27}H_{41}NO_5$	460.3065	460.3063	0.2	460.3065 [M + H]$^+$; 442.2870 [M + H-H_2O]$^+$; 424.0822 [M + H-2H_2O]$^+$	15β-hydroxy-23-isopengbeisine B or verdine	A	PBM
9	2.74	[M + H]$^+$	$C_{27}H_{43}NO_6$	478.3171	478.3169	0.4	478.3171 [M + H]$^+$; 460.3003 [M + H-H_2O]$^+$; 442.2882 [M + H-2H_2O]$^+$	pingbeimine C	A	PBM
10	3.15	[M−H]$^-$	$C_{26}H_{28}O_{14}$	563.1403	563.1401	0.4	563.1403 [M−H]$^-$; 473.1078 [M−H−$C_3H_6O_3$]$^-$; 443.1001 [M−H−$C_3H_6O_3$−CH_2O]$^-$; 383.0754 [M−H−2$C_3H_6O_3$]$^-$; 353.0668 [M−H−2$C_3H_6O_3$−CH_2O]$^-$	schaftoside	F	GC
11	3.19	[M−H]$^-$	$C_{26}H_{28}O_{14}$	563.1403	563.1401	0.4	563.1403 [M−H]-; 473.1065 [M−H−$C_3H_6O_3$]$^-$; 443.0986 [M−H−$C_3H_6O_3$−CH_2O]$^-$; 383.0779 [M−H−2$C_3H_6O_3$]$^-$; 353.0668 [M−H−2$C_3H_6O_3$−CH_2O]$^-$	isoschaftoside	F	GC
12	3.59	[M + H]$^+$	$C_{33}H_{51}NO_8$	590.3694	590.3693	0.2	590.3694 [M + H]$^+$; 572.3615 [M + H-H_2O]$^+$	(20R,25R)−23,26-epimino-3β-hydroxy-5α-cholest-23(N)-ene-6,22-dione-3-O-β-ᴅ-glucopyranoside	A	PBM
13*	3.65	[M−H]$^-$	$C_{21}H_{20}O_{10}$	431.0970	431.0978	−1.9	431.0970 [M−H]$^-$; 269.0445 [M−H−Glu]$^-$	aloeemodin-8-O-β-D-glucopyranoside	AN	DH
14	3.66	[M−H]$^-$	$C_{26}H_{30}O_{13}$	549.1605	549.1608	−0.4	549.1605 [M−H]$^-$; 417.1778 [M−H−$C_5H_8O_4$]$^-$; 255.0655 [M−H−$C_5H_8O_4$−Glu]-	isoliquirtin apioside	F	GC
15*	3.75	[M−H]$^-$	$C_{26}H_{30}O_{13}$	549.1617	549.1608	1.6	549.1617 [M−H]$^-$; 417.1776 [M−H−$C_5H_8O_4$]$^-$; 255.0635 [M−H−$C_5H_8O_4$−Glu]$^-$	liquiritigenin apioside	F	GC
16*	3.80	[M−H]$^-$	$C_{21}H_{22}O_9$	417.1182	417.1186	−1.0	417.1182 [M−H]$^-$; 255.0658 [M−H−Glc]$^-$;135.0086 [$^{1,3}A_0$]$^-$;119.0497 [$^{1,3}B_0$]$^-$	liquiritin	F	GC
17	4.04	[M + H]$^+$	$C_{27}H_{38}NO_3$	424.2852	424.2860	−0.8	424.2852 [M + H]$^+$; 406.0642 [M + H-H_2O]$^+$	ussuriedine	A	PMB
18	4.12	[M−H]$^-$	$C_{26}H_{28}O_{13}$	547.1466	547.1452	2.6	547.1466 [M−H]$^-$; 457.1129 [M−H−$C_3H_6O_3$]$^-$; 427.1027 [M−H−$C_3H_6O_3$−CH_2O]$^-$; 367.0843 [M−H−2$C_3H_6O_3$]$^-$; 337.0788 [M−H−2$C_3H_6O_3$−CH_2O]$^-$	chrysin6-C-β-ᴅ-glucopyranosyl-8-C-α-ʟ-arabinopyranoside	F	HQ
19	4.22	[M−H]$^-$	$C_{26}H_{28}O_{13}$	547.1458	547.1452	1.1	547.1458 [M−H]$^-$; 457.1130 [M−H−$C_3H_6O_3$]$^-$; 427.1030 [M−H−$C_3H_6O_3$−CH_2O]$^-$; 367.0817 [M−H−2$C_3H_6O_3$]$^-$; 337.0702 [M−H−2$C_3H_6O_3$−CH_2O]$^-$	chyrsin-6-C-α-ʟ-arabinopyranosyl-8-C-β-ᴅ-glucopyranoside	F	HQ
20	4.37	[M + H]$^+$	$C_{33}H_{54}NO_8$	592.3845	592.3847	−0.2	592.3845 [M + H]$^+$; 574.3664 [M + H-H_2O]$^+$	zhebeinone-3-β-ᴅ-glucoside	A	PMB
21	4.57	[M−H]$^-$	$C_{22}H_{20}O_{12}$	475.0876	475.0877	−0.2	475.0876 [M−H]$^-$; 299.0545 [M−H−GluA]$^-$	diosmetin-7-O-β-ᴅ-glucuronide	F	HQ
22	4.66	[M−H]$^-$	$C_{21}H_{20}O_9$	415.1029	415.1029	0.0	415.1029 [M−H]$^-$; 253.0434[M-H-Glu]$^-$;239.0428[M-H-Glu-CH_2]$^-$ 225.0550[M-H-Glu-CO]$^-$	pulmatin	AN	DH
23*	4.75	[M + H]$^+$	$C_{27}H_{41}NO_3$	428.3167	428.3165	0.2	428.3167 [M + H]$^+$; 410.3097 [M + H-H_2O]$^+$; 393.2801 [M + H-H_2O-NH_3]$^+$	peimisine	A	PBM
24	4.97	[M + H]$^+$	$C_{27}H_{45}NO_3$	432.3467	432.3478	−2.5	432.3467 [M + H]$^+$; 414.3371 [M + H-H_2O]$^+$	verticine	A	PBM

(continued on next page)

Table 1 (*continued*)

No	t_R	Selected ion	Elemental Composition	Measured mass	Calculated mass	Mass error	Fragmentations (*m/z*)	Identification or tentative characterization	Type	Source[a]
25	5.12	[M−H]⁻	$C_{22}H_{20}O_{12}$	475.0874	475.0877	−0.6	475.0874 [M−H]⁻; 299.0540 [M−H−GluA]⁻; 284.0377 [M−H−GluA−CH$_3$]⁻	hispidalin-7-*O*-β-ᴅ-glucuronide	F	HQ
26	5.38	[M−H]⁻	$C_{26}H_{30}O_{13}$	549.1608	549.1608	0.0	549.1608 [M−H]⁻; 417.1788 [M−H−Api]⁻; 255.0656 [M−H−Api−Glc]⁻	liquiritigenin-7-*O*-β-ᴅ-apiosyl-4′-*O*-β-ᴅ-glucoside	F	GC
27*	5.45	[M + H]⁺	$C_{27}H_{43}NO_3$	430.3319	430.3321	−0.5	430.3319 [M + H]⁺; 412.3211 [M + H-H$_2$O]⁺; 396.2971 [M + H-H$_2$O-CH$_4$]⁺	peiminine	A	PBM
28	5.55	[M + H]⁺	$C_{32}H_{52}NO_8$	578.3701	578.3693	0.8	578.3701 [M + H]⁺; 560.3484 [M + H-H$_2$O]⁺; 164.1428 [M + H-C$_{21}$H$_{34}$O$_8$]⁺	pingbeinone-3-*O*-β-ᴅ-glucoside	A	PBM
29*	5.69	[M−H]⁻	$C_{21}H_{22}O_9$	417.1180	417.1186	−1.4	417.1180 [M−H]⁻; 255.0657 [M−H−Glc]⁻; 135.0086 [^{1,3}A$_0$]⁻; 119.0508 [^{1,3}B$_0$]⁻	isoliquiritin	F	GC
30*	6.10	[M−H]⁻	$C_{21}H_{18}O_{11}$	445.0770	445.0771	−0.2	891.1619 [2 M−H]⁻;445.0770 [M−H]⁻; 269.0447 [M−H−GluA]⁻; 251.0341 [M−H−GluA−H$_2$O]⁻; 241.0508 [M−H−GluA−CO]⁻; 223.0401 [M−H−GluA−H$_2$O−CO]⁻; 195.0452 [M−H−GluA−H$_2$O−2CO]⁻; 175.0249 [M-H-C$_{15}$H$_{10}$O$_5$]⁻; 113.0236 [M−H-C$_{16}$H$_{12}$O$_8$]⁻	baicalin	F	HQ
31	6.20	[M−H]⁻	$C_{21}H_{18}O_{11}$	445.0775	445.0771	0.9	445.0771 [M−H]⁻; 269.0450 [M−H−GluA]⁻; 251.0342 [M−H−GluA−H$_2$O]⁻; 223.0353 [M−H−GluA−H$_2$O−CO]⁻;195.0462 [M−H−GluA−H$_2$O−2CO]⁻	baicalein-6-*O*-β-ᴅ-glucuronide	F	HQ
32*	6.24	[M−H]⁻	$C_{15}H_{12}O_4$	255.0657	255.0657	0.0	255.0657 [M−H]⁻; 135.0080[^{1,3}A$_0$]⁻; 119.0503 [^{1,3}B$_0$]⁻	liquiritigenin	F	GC
33	6.30	[M−H]⁻	$C_{22}H_{20}O_{11}$	459.0930	459.0927	0.7	459.0930 [M−H]⁻; 269.0460 [M−H−methylgluA]⁻; 251.0334 [M−H−methylgluA−H$_2$O]⁻; 241.0487 [M−H−methylgluA−CO]⁻; 223.0398 [M−H−methylgluA−H$_2$O−CO]⁻; 197.0571 [M−H−methylgluA−CO−CO$_2$]⁻;	baicalein-7-*O*-glucuronide-methyl ester	F	HQ
34	6.60	[M + H]⁺	$C_{26}H_{42}NO_3$	416.3155	416.3175	−2.0	416.3155 [M + H]⁺; 398.3002[M + H-H$_2$O]⁺; 163.1315 [M + H-C$_{15}$H$_{25}$O$_3$]⁺;	pingbeinone	A	PBM
35	7.13	[M−H]⁻	$C_{21}H_{18}O_{11}$	445.0762	445.0771	−2.0	445.0762 [M + H]⁺; 269.0456 [M−H−GluA]⁻; 251.0352 [M−H−GluA−H$_2$O]⁻; 241.0459 [M−H−GluA−CO]⁻; 223.0352 [M−H−GluA−H$_2$O−CO]⁻; 195.0460 [M−H−GluA−H$_2$O−2CO]⁻	apigenin-7-*O*-β-ᴅ-glucronide	F	HQ
36	7.33	[M−H]⁻	$C_{21}H_{18}O_{11}$	445.0769	445.0771	−0.4	445.0769 [M−H]⁻; 269.0473[M-H-GluA]⁻	norwogonin-7-*O*-β-ᴅ-glucuronide	F	HQ
37	7.48	[M−H]⁻	$C_{22}H_{20}O_{12}$	475.0871	475.0877	−1.3	475.0871 [M−H]⁻; 299.0540 [M−H−GluA]⁻; 284.0377[M-H-GluA-CH$_3$]⁻	scutevurin-7-*O*-β-ᴅ-glucuronide	F	HQ
38*	7.73	[M−H]⁻	$C_{21}H_{18}O_{10}$	429.0826	429.0822	0.9	429.0826 [M−H]⁻; 253.0500 [M−H−GluA]⁻; 209.0613 [M−H−GluA−CO$_2$]⁻; 151.0046 [^{1,3}A$_0$]⁻	chrysin 7-*O*-β-ᴅ-glucuronide	F	HQ
39*	7.79	[M−H]⁻	$C_{22}H_{20}O_{11}$	459.0935	459.0927	1.7	919.1959 [2 M−H]⁻; 459.0935 [M−H]⁻; 283.0612 [M−H−GluA]⁻; 268.0377 [M−H−GluA−CH$_3$]⁻; 240.0412 [M−H−GluA−CH$_3$−CO]⁻	oroxylin A 7-*O*-β-ᴅ-glucuronide	F	HQ
40*	7.83	[M−H]⁻	$C_{21}H_{20}O_9$	415.1041	415.1029	2.9	415.1041 [M−H]⁻; 295.0607 [M−H−C$_4$H$_8$O$_4$]⁻; 277.0515 [M−H−C$_4$H$_8$O$_4$−H$_2$O]⁻; 253.0503 [M−H−Glu]⁻; 225.0560 [M−H−Glu−CO]⁻	chrysophanol-1-*O*-β-ᴅ-glucopyranoside	AN	DH
41	7.98	[M−H]⁻	$C_{22}H_{20}O_{12}$	475.0877	475.0877	0.0	475.0877 [M−H]⁻; 284.0377 [M−H−methylester]⁻	scutellarin methyl ester	F	HQ
42	8.05	[M−H]⁻	$C_{21}H_{20}O_{10}$	431.0986	431.0978	1.9	431.0986 [M−H]⁻; 269.0442 [M−H−Glu]⁻; 151.0028 [^{1,3}A$_0$]⁻	apigenin 7-*O*-β-ᴅ-glucoside	F	GC
43*	8.08	[M−H]⁻	$C_{21}H_{20}O_{10}$	431.0976	431.0978	−0.5	431.0976 [M−H]⁻; 269.0445 [M−H−Glu]⁻; 241.0506 [M−H−Glu−CO]⁻; 223.0416 [M−H−Glu−CO−H$_2$O]⁻	baicalin 7-*O*-β-ᴅ-glucoside	F	HQ
44	8.15	[M−H]⁻	$C_{21}H_{18}O_{11}$	445.0763	445.0771	−1.8	445.0763 [M−H]⁻; 283.0605 [M−H−Glu]⁻; 239.0341 [M−H−Glu−CO$_2$]⁻; 211.0388 [M−H−Glu−CO$_2$−CO]⁻; 183.0446 [M−H−Glu−CO$_2$−2CO]⁻	rhein-8-*O*-β-ᴅ-glucoside	AN	DH

Table 1 (*continued*)

No	t_R	Selected ion	Elemental Composition	Measured mass	Calculated mass	Mass error	Fragmentations (*m/z*)	Identification or tentative characterization	Type	Source[a]
45*	8.22	[M−H]⁻	$C_{21}H_{20}O_9$	415.1025	415.1029	−1.0	415.1025 [M−H]⁻; 295.0605 [M−H−$C_4H_8O_4$]⁻; 277.0512 [M−H−$C_4H_8O_4$−H_2O]⁻; 253.0507 [M−H−Glu]⁻; 225.0550 [M−H−Glu−CO]⁻	chrysophanol-8-*O*-*β*-D-glucopyranoside	AN	DH
46*	8.31	[M−H]⁻	$C_{22}H_{20}O_{11}$	459.0934	459.0927	1.5	919.1932 [2 M−H]⁻; 459.0934 [M−H]⁻; 283.0599 [M−H−GluA]⁻; 268.0378 [M−H−GluA−CH_3]⁻;240.0417 [M−H−GluA−CH_3−CO]⁻; 175.0248 [M−H−$C_{16}H_{12}O_5$]⁻; 163.0035 [M−H−$C_{14}H_{16}O_7$]⁻; 113.0241 [M−H−$C_{16}H_{12}O_5$−CO_2−H_2O]⁻	wogonoside	F	HQ
47	8.48	[M−H]⁻	$C_{22}H_{22}O_{11}$	461.1084	461.1084	0.0	461.1084 [M−H]⁻; 315.0685 [M−H−$C_9H_7O_2$]⁻; 313.0798 [M−H−$C_9H_7O_2$−2H]⁻	2-*O*-cinnamoyl-glucogallin	O	DH
48	8.76	[M−H]⁻	$C_{44}H_{64}O_{19}$	895.3960	895.3964	−0.3	895.3960 [M−H]⁻; 837.3891 [M−H−$C_2H_2O_2$]⁻	22β-acetoxyl licorice saponin G2	T	GC
49	9.00	[M−H]⁻	$C_{44}H_{70}O_{23}$	965.4227	965.4230	−0.3	965.4230 [M−H]⁻; 803.3706 [M−H−Glc]⁻;641.3164 [M−H−2Glc]⁻	rebaudioside A	D	FL
50*	9.08	[M−H]⁻	$C_{38}H_{60}O_{18}$	803.3707	803.3701	0.6	803.3707 [M−H]⁻; 641.3176 [M−H−Glc]⁻; 479.2609 [M−H−2Glc]⁻	stevioside	D	FL
51	9.33	[M−H]⁻	$C_{26}H_{45}NO_7S$	514.2843	514.2838	1.0	514.2843 [M−H]⁻	taurocholic acid	B	RGNH
52	9.40	[M−H]⁻	$C_{16}H_{12}O_5$	935.4132	935.4124	0.9	935.4132 [M−H]⁻; 283.0602 [M−H−3Glc−Xyl]⁻	rebaudioside B xyloside	D	FL
53	9.52	[M−H]⁻	$C_{44}H_{70}O_{22}$	949.4291	949.4280	1.2	949.4291 [M−H]⁻; 787.3871 [M−H−Glc]⁻; 625.3272 [M−H−2Glc]⁻	rebaudioside C	D	FL
54*	9.69	[M−H]⁻	$C_{15}H_{12}O_4$	255.0649	255.0657	−3.1	255.0649 [M−H]⁻; 119.0503 [$^{1,3}B_0$]⁻	isoliquiritigenin	F	GC
55	9.74	[M−H]⁻	$C_{38}H_{60}O_{18}$	803.3693	803.3701	−1.0	849.3749 [M−H + HCOOH]⁻; 803.3693 [M−H]⁻; 641.3174 [M−H−Glc]⁻; 479.2610 [M−H−2Glc]⁻	rebaudioside G	D	FL
56	9.77	[M−H]⁻	$C_{42}H_{62}O_{17}$	837.3904	837.3909	−0.6	837.3904 [M−H]⁻; 485.3302 [M−H−2GulA]⁻; 351.0554 [M−H−$C_{30}H_{46}O_5$]⁻; 193.0357 [M−H−$C_{36}H_{52}O_{10}$]⁻	licorice-saponin P2	T	GC
57	10.07	[M + H]⁺	$C_{16}H_{12}O_4$	269.0816	269.0814	0.7	269.0816 [M + H]⁺	formononetin	F	GC
58	10.42	[M−H]⁻	$C_{16}H_{10}O_6$	297.0400	297.0399	0.3	297.0400 [M−H]⁻; 253.0497 [M−H−CO_2]⁻	glyzaglabrin	F	GC
59	10.47	[M−H]⁻	$C_{42}H_{60}O_{16}$	819.3802	819.3803	−0.1	819.3802 [M−H]⁻; 351.0555 [M−H−$C_{30}H_{44}O_4$]⁻	licorice-saponin E₂	T	GC
60*	10.49	[M−H]⁻	$C_{42}H_{62}O_{17}$	837.3914	837.3909	0.6	837.3914 [M−H]⁻; 351.0561 [M−H−$C_{30}H_{46}O_5$]⁻	licorice-saponin G2	T	GC
61	10.60	[M−H]⁻	$C_{32}H_{50}O_{13}$	641.3170	641.3173	−0.5	641.3170 [M−H]⁻; 479.2609 [M−H−Glc]⁻	steviobioside	D	FL
62	10.72	[M + H]⁺	$C_{26}H_{43}NO_6$	466.3169	466.3169	0.0	931.6238 [2 M + H]⁺; 466.3169 [M + H]⁺; 448.3058 [M + H-H_2O]⁺; 430.2952 [M + H-2H_2O]⁺; 412.2847 [M + H-3H_2O]⁺; 337.2531 [M + H-3H_2O-$C_2H_5NO_2$]⁺	glycocholic acid	B	RGNH
63	10.77	[M−H]⁻	$C_{42}H_{62}O_{17}$	837.3921	837.3909	1.4	837.3921 [M−H]⁻	uralsaponin U	T	GC
64	10.82	[M−H]⁻	$C_{38}H_{60}O_{17}$	787.3761	787.3752	1.1	787.3761 [M−H]⁻; 625.3240 [M−H−Glc]⁻	dulcosideA	D	FL
65	10.96	[M−H]⁻	$C_{26}H_{45}NO_6S$	498.2889	498.2889	0.0	498.2889 [M−H]⁻	taurodeoxycholic acid	B	RGNH
66	11.10	[M + H]⁺	$C_{42}H_{62}O_{16}$	823.4115	823.4116	−0.5	823.4115 [M + H]⁺; 647.3783 [M + H-GluA]⁺; 453.3377 [M + H-2GluA-H_2O]⁺	licorice-saponin K₂	T	GC
67*	11.16	[M + H]⁺	$C_{42}H_{62}O_{16}$	823.4118	823.4116	0.2	823.4118 [M + H]⁺; 805.3953 [M + H-H_2O]⁺; 647.3783 [M + H-GluA]⁺; 471.3643 [M + H-2GluA]⁺; 453.3363 [M + H-2GluA-H_2O]⁺; 435.3257 [M + H-2GluA-2H_2O]⁺; 407.3294 [M + H-2GluA-2H_2O-CO]⁺; 285.2221 [M + H-2GluA-2H_2O-CO-C_9H_{14}]⁺; 189.1645 [M + H-2GluA-2H_2O-CO-C_9H_{14}-C_5H_8O]⁺	glycyrrhizic acid	T	GC
68*	11.25	[M−H]⁻	$C_{15}H_8O_6$	283.0239	283.0243	−0.2	283.0239 [M−H]⁻; 239.0344 [M−H−CO_2]⁻; 211.0388 [M−H−CO_2−CO]⁻; 183.0446 [M−H−CO_2−2CO]⁻	rhein	AN	DH
69	11.27	[M−H]⁻	$C_{26}H_{45}NO_6S$	498.2898	498.2889	1.8	498.2898 [M−H]⁻	taurochenodeoxycholic acid	B	RGNH
70*	11.32	[M−H]⁻	$C_{16}H_{12}O_5$	283.0608	283.0606	0.2	283.0606 [M−H]⁻; 268.0365[M-H-CH_3]⁻;240.0413[M-H-CH_3-CO]⁻;	wogonin	F	HQ

Table 1 (*continued*)

No	t_R	Selected ion	Elemental Composition	Measured mass	Calculated mass	Mass error	Fragmentations (*m/z*)	Identification or tentative characterization	Type	Source[a]
71	11.40	$[M-H]^-$	$C_{42}H_{64}O_{15}$	807.4149	807.4167	−1.6	239.0336[M-H-CH$_4$-CO]$^-$;212.04553 [M-H-CH$_3$-CO-H$_2$O]$^-$ 807.4149 [M−H]$^-$; 351.0558 [M−H−C$_{30}$H$_{48}$O$_3$]$^-$; 193.0343 [M−H−C$_{36}$H$_{54}$O$_8$]$^-$	licorice-saponin B2	T	GC
72	11.46	$[M-H]^-$	$C_{15}H_{10}O_4$	253.0493	253.0501	0.3	253.0493 [M−H]$^-$; 225.0565 [M−H−CO]$^-$; 209.0600[M-H-CO$_2$]$^-$; 181.0699 [M−H−CO−CO$_2$]$^-$; 153.0745[M-H-2CO-CO$_2$]$^-$	chrysin	F	HQ
73	11.60	$[M-H]^-$	$C_{24}H_{40}O_5$	407.2793	407.2797	−1.0	407.2793 [M−H]$^-$; 389.2767 [M−H−H$_2$O]$^-$; 371.2608 [M−H−2H$_2$O]$^-$; 353.2482 [M−H−3H$_2$O]$^-$; 345.2792 [M−H−CO$_2$−H$_2$O]$^-$	allocholic acid	B	RGNH
74*	11.77	$[M-H]^-$	$C_{19}H_{18}O_8$	373.0931	373.0923	2.1	373.0931 [M−H]$^-$; 358.0697 [M−H−CH$_3$]$^-$; 343.0466 [M−H−2CH$_3$]$^-$; 328.0220 [M−H−3CH$_3$]$^-$; 313.0011 [M−H−4CH$_3$]$^-$	skullcapflavone II	F	HQ
75*	11.85	$[M + H]^+$	$C_{42}H_{62}O_{16}$	823.4099	823.4116	−2.1	823.4009 [M + H]$^+$; 647.3802 [M + H-GluA]$^+$; 453.3364 [M + H-2GluA-H$_2$O]$^+$; 263.1619 [M + H-2GluA-H$_2$O-C$_{14}$H$_{22}$]$^+$; 191.1812 [M + H-2GluA-H$_2$O-C$_{16}$H$_{22}$O$_3$]$^+$	(18β, 20α)-glycyrrhizic acid	T	GC
76	12.05	$[M-H]^-$	$C_{24}H_{40}O_5$	407.2795	407.2797	−0.5	407.2795 [M−H]$^-$; 389.2698 [M−H−H$_2$O]$^-$; 371.2572 [M−H−2H$_2$O]$^-$	hyocholic acid	B	RGNH
77	12.08	$[M + H]^+$	$C_{42}H_{62}O_{16}$	823.4100	823.4116	−1.9	823.4100 [M + H]$^+$; 647.3790 [M + H-GluA]$^+$; 453.3354 [M + H-2GluA-H$_2$O]$^+$	uralsaponin B	T	GC
78*	12.19	$[M-H]^-$	$C_{24}H_{40}O_5$	407.2794	407.2797	−0.7	815.5669[2 M−H]$^-$; 407.2794 [M−H]$^-$; 389.2696 [M−H−H$_2$O]$^-$; 371.2601 [M−H−2H$_2$O]$^-$; 353.2473 [M−H−3H$_2$O]$^-$; 345.2807 [M−H−CO$_2$−H$_2$O]$^-$; 343.2636 [M−H−2H−CO$_2$−H$_2$O]$^-$; 327.2683 [M−H−CO$_2$−2H$_2$O]$^-$; 325.2518 [M−H−2H−CO$_2$−2H$_2$O]$^-$; 289.2173 [M−H$_2$O−C$_5$H$_8$O$_2$]$^-$	cholic acid	B	RGNH
79*	12.46	$[M-H]^-$	$C_{24}H_{40}O_4$	391.2850	391.2848	0.5	783.5778 [2 M−H]$^-$; 391.2850 [M−H]$^-$;373.2743 [M−H−H$_2$O]$^-$; 355.0060 [M−H−2H$_2$O]$^-$; 328.9925 [M−H−CO$_2$−H$_2$O]$^-$	hyodeoxycholic acid	B	RGNH
80	12.56	$[M-H]^-$	$C_{42}H_{64}O_{16}$	823.4114	823.4116	−0.2	823.4114 [M−H]$^-$; 351.0561 [2GluA]$^-$	uralsaponin C	T	GC
81	12.68	$[M-H]^-$	$C_{21}H_{24}O_5$	355.1548	355.1545	0.8	711.3177 [2 M−H]$^-$; 355.1548 [M−H]$^-$	glyasperin C	F	GC
82	12.82	$[M + H]^+$	$C_{26}H_{43}NO_5$	450.3228	450.3219	0.2	450.3228 [M + H]$^+$; 414.3009 [M + H-2H$_2$O]$^+$; 339.2680 [M + H-2H$_2$O-C$_2$H$_5$NO$_2$]$^+$	glycohyodeoxycholic acid	B	RGNH
83	13.16	$[M-H]^-$	$C_{20}H_{18}O_6$	353.1024	353.1025	−0.3	353.1024 [M−H]$^-$	licoflavonol	F	GC
84	13.24	$[M-H]^-$	$C_{42}H_{62}O_{16}$	821.3979	821.3960	2.3	821.3979 [M−H]$^-$; 351.0574 [M−H−C$_{30}$H$_{46}$O$_4$]$^-$; 193.0386 [M−H−C$_{36}$H$_{52}$O$_9$]$^-$	licorice-saponin H$_2$	T	GC
85	13.51	$[M-H]^-$	$C_{42}H_{64}O_{16}$	823.4111	823.4116	−0.6	823.4111 [M−H]$^-$; 351.0869 [M−H−C$_{30}$H$_{48}$O$_4$]$^-$	licorice-saponin J$_2$	T	GC
86	13.54	$[M-H]^-$	$C_{22}H_{22}O_6$	381.1330	381.1336	−0.8	381.1330 [M−H]$^-$; 351.0880 [M−H−CH$_2$O]$^-$; 323.0558 [M−H−CH$_2$O−CO]$^-$	licoricone	F	GC
87	13.65	$[M-H]^-$	$C_{15}H_{10}O_5$	269.0446	269.0450	0.3	269.0446 [M−H]$^-$; 251.0382 [M−H−H$_2$O]$^-$; 241.0497 [M−H−CO]$^-$; 225.0540 [M−H−CO$_2$]$^-$; 197.0602 [M−H−CO$_2$−CO]$^-$; 195.0467 [M−H−2CO−H$_2$O]$^-$	baicalein	F	HQ
88*	14.27	$[M-H]^-$	$C_{24}H_{40}O_4$	391.2848	391.2848	0.0	783.5778 [2 M−H]$^-$; 391.2848 [M−H]$^-$; 373.2743[M-H-H$_2$O]$^-$; 355.0060 [M−H−2H$_2$O]$^-$; 328.9925 [M-H-CO$_2$-H$_2$O]$^-$	chenodeoxycholic acid	B	RGNH
89	14.37	$[M-H]^-$	$C_{20}H_{16}O_6$	351.0867	351.0869	−0.6	351.0867 [M−H]$^-$	licoisoflavone B	F	GC
90*	14.44	$[M-H]^-$	$C_{24}H_{40}O_4$	391.2851	391.2848	0.8	783.5765 [2 M−H]$^-$; 391.2851 [M−H]$^-$; 373.2748 [M−H−H$_2$O]$^-$; 355.0062 [M−H−2H$_2$O]$^-$; 328.9931 [M−H−CO$_2$−H$_2$O]$^-$	deoxycholic acid	B	RGNH
91	14.89	$[M-H]^-$	$C_{22}H_{26}O_5$	369.1700	369.1702	−0.2	369.1700 [M−H]$^-$; 341.1080 [M−H−CO]$^-$	glyasperin D	F	GC
92*	15.46	$[M-H]^-$	$C_{30}H_{46}O_4$	469.3325	469.3318	0.7	469.3325 [M−H]$^-$; 433.2961 [M−H−2H$_2$O]$^-$	glycyrrhetinic acid	T	GC

Note: * the compound was unambiguously identified with reference standard, F: Flavonoids, T: Triterpenoid saponins, A: Alkaloids, B: Bile acids, AN: Anthraquinones, D: Diterpenoids, O: Others.

[a] Scutellariae Radix (Huangqin, HQ), Fritillariae Ussuriensis Bulbus (Pingbeimu, PBM), Rhei Radix et Rhizoma (Dahuang, DH), Bovis Calculus Artifactus (Rengongniuhuang, RGNH), Glycyrrhizae Radix et Rhizoma (Gancao, GC) and excipient (Fuliao, FL) are abbreviated as HQ, PBM, DH, RGNH, GC, and FL.
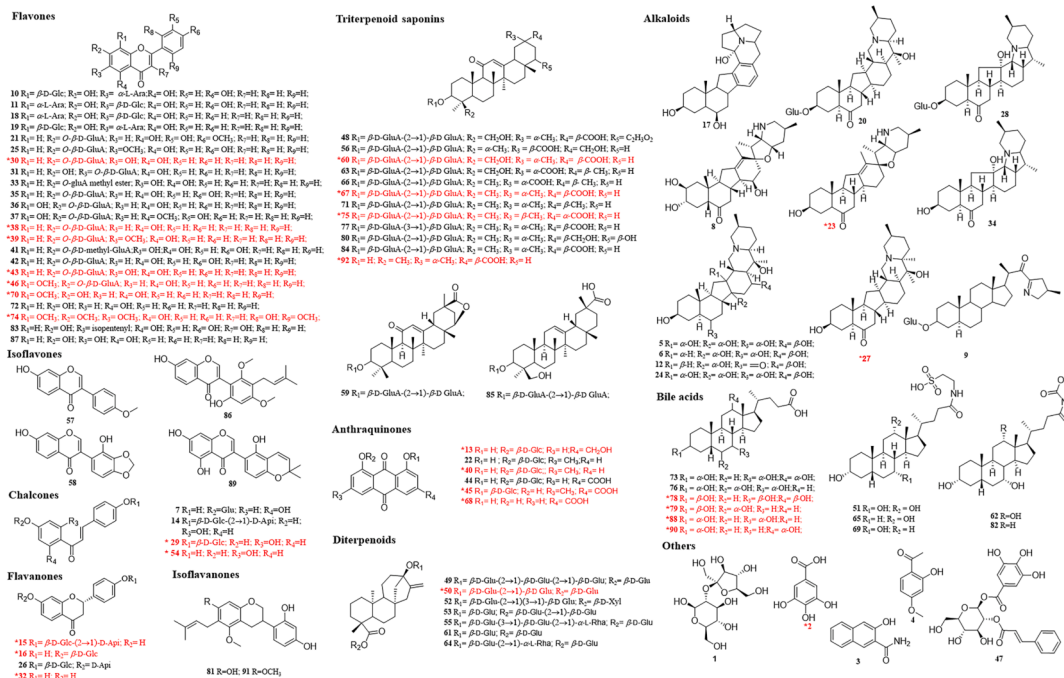
Fig. 2. Chemical structures of components identified or characterized in JZOL (red color represented the confirmed compounds by comparison with reference standards). (For interpretation of the references to color in this figure legend, the reader is referred to the web version of this article.)
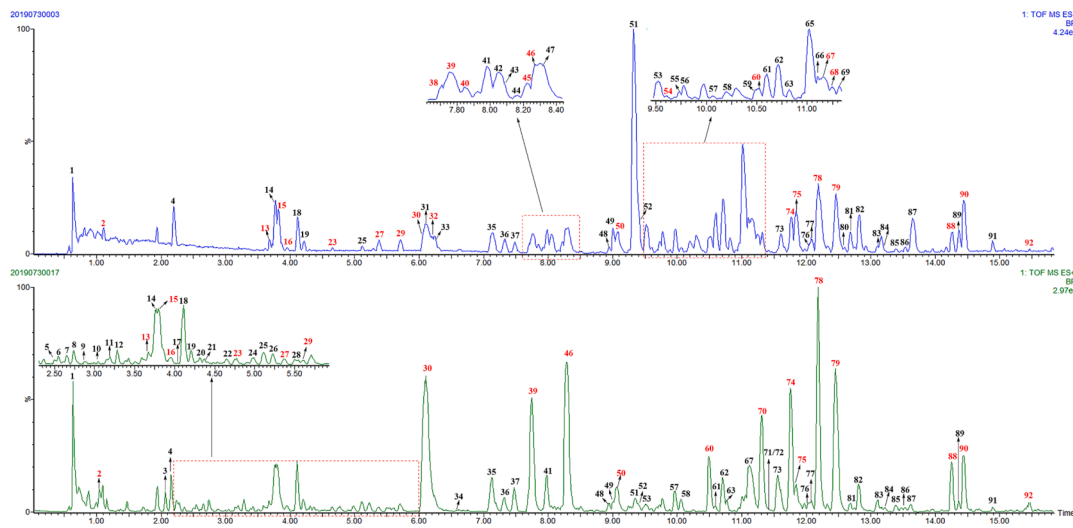
Fig. 3. The basic peak ions chromatography of JZOL detected by UPLC-Q/TOF-MS (red color represented the confirmed compounds by comparison with reference standards). (For interpretation of the references to color in this figure legend, the reader is referred to the web version of this article.)

3.2. Method validation of pharmacokinetic research

Based on the analysis of exogenous substances by JZOL in rats, 21 accurately identified prototype components were detected in rat plasma (Zhang et al., 2022, **Table S3**), 11 of which showed high exposure and covered different structural types of the compounds. These compounds included baicalin (flavonoids), wogonoside (flavonoids), wogonin (flavonoids) and oyoxylin A-7-*O*-*β*-D-gluA (flavonoids) from Scutellariae Radix, liquiritin (flavonoids), liquiritigenin (flavonoids),

isoliquiritigenin (flavonoids), isoliquiritin (flavonoids), glycyrrhizic acid (triterpenoid saponins) from Glycyrrhizae Radix et Rhizoma, rhein from Rhei Radix et Rhizoma, and peimisine (alkaloids) from Fritillariae Ussuriensis Bulbus.

A set of method validation tests of 11 analytes (**Fig. S5**) were conducted in the matrix, including specificity and selectivity, standard curve and linear range, precision and accuracy, extraction recovery and matrix effect, and stability. Specificity testing demonstrated no or negligible chromatographic interference to the analytes (**Fig. S6**). All
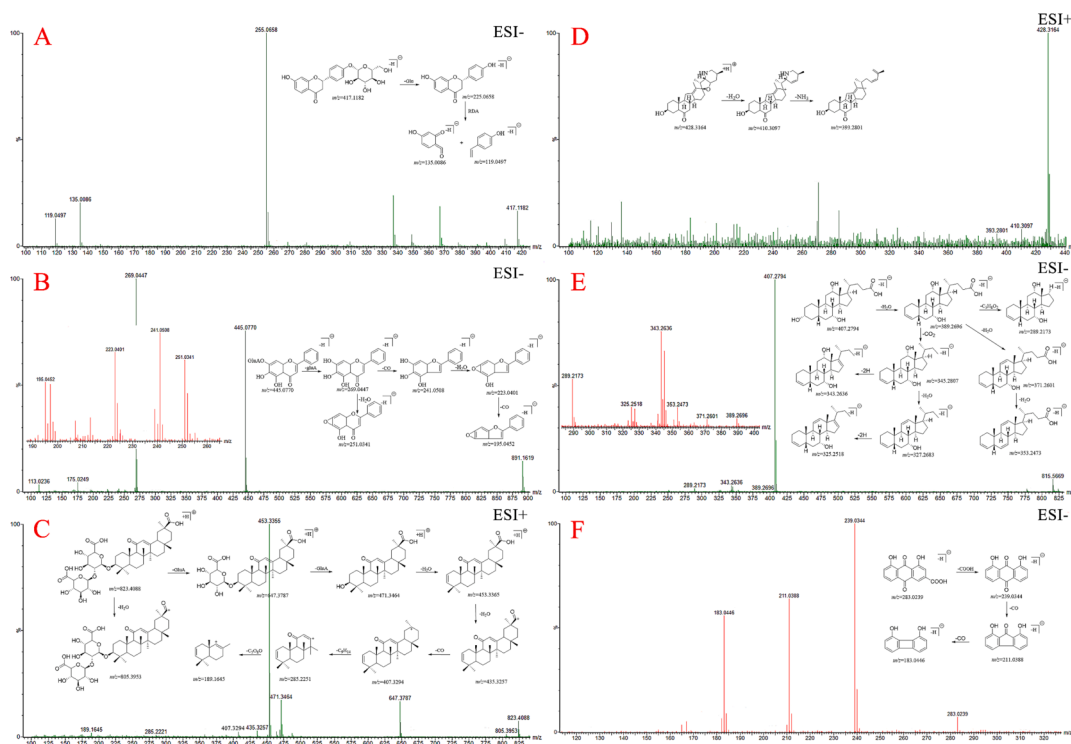
Fig. 4. The detailed fragmentation and proposed fragment pathways of compounds (A) **16**-liquiritin; (B) **30**-baicalin; (C) **67**-glycyrrhizic acid; (D) **23**-peimisine; (E) **78**- cholic acid; (F) **68**-rhein.

analytes exhibited good linearity (r ≥ 0.99) within the test ranges (**Table S5**), and both the accuracy (RE: 3.33 %-8.68 %) and precision (RSD: −2.32 %-2.16 %) of the LLOQ met the requirements of the guidelines (**Table S6**), indicating that the established method was sufficiently sensitive for quantifying the 11 analytes in rat plasma. As shown in **Table S7**, the values of intra- and inter-day precision at three concentrations (LQC, MQC, HQC) were less than 15 %. And the accuracy (RE%) of 11 analytes ranged between −10.16 % to 14.05 % for intra-day and −7.51 %–10.01 % for inter-day, demonstrating satisfactory precision and accuracy for pharmacokinetic studies. The recoveries of the analytes varied from 84.79 % to 107.94 % (glycyrrhizic acid: 10.79 %) and the recovery of IS was 100.74 %, illustrating consistent recovery and precision (**Table S8**). The matrix effects of the analytes ranged from 85.46 % to 111.97 % with RSDs within 8.94 %, indicating no remarkable matrix effect in rat plasma (**Table S8**). The carry-over effect was negligible in this method, as insignificant peaks were observed in each channel of the blank plasma sample after ULOQ (**Fig. S7**). The RSD values of stability under different conditions (free-thaw cycles, room temperature for 8 h, −80 °C for 2 weeks, MS Auto–sampler for 24 h) were less than 12.54 % (**Table S9**), indicating that the analytes remained stable under analytical conditions. The summarized results prove the validity of the developed UPLC-MS/MS method for the pharmacokinetic analysis of 11 ingredients in rat plasma.

3.3. Pharmacokinetic studies

The validated UPLC-MS/MS method for analyzing 11 components in rat plasma was applied for the pharmacokinetic study following JZOL oral administration. The mean plasma concentration–time profiles of the 11 detected prototypes are shown in **Fig. 5**. Statistical analysis of the pharmacokinetic parameters was performed with WinNonlin 6.3 software, and the corresponding estimated pharmacokinetic parameters ($t_{1/2}$, T_{max}, C_{max}, $AUC_{0-\infty}$, AUC_{0-t}, $MRT_{0-\infty}$, MRT_{0-t}) are given in **Table 2**.

According to the pharmacokinetic profiles of the 11 ingredients from JZOL, the $t_{1/2}$ value was in the range of 1.39–50.93 h. Liquiritin,

wogonoside, oroxylin A 7-O-β-D-glucuronide and baicalin were rapidly absorbed, with high C_{max} values (138.02 ± 40.22, 343.88 ± 223.12, 98.97 ± 63.50 and 1134.15 ± 550.36 ng/mL) and high $AUC_{0-\infty}$ values (1086.90 ± 344.28, 3685.52 ± 869.65, 2164.23 ± 1398.77 and 9650.72 ± 5013.90 ng*h*mL^{-1}), indicating high exposure and peak concentrations in blood. The C_{max} values of wogonin, isoliquiritigenin, liquiritigenin, and isoliquiritigenin ranged from 1.67 to 8.73 ng/mL. Among them, isoliquiritigenin and liquiritigenin exhibited two peaks in the pharmacokinetic profile.

Rhein derived from Rhei Radix et Rhizoma demonstrated rapid but poor absorption from the gastrointestinal tract (T_{max} = 0.42 ± 0.13 h, $t_{1/2}$ = 9.86 ± 2.73 h, C_{max} = 18.98 ± 7.19 ng/mL, $AUC_{0-\infty}$=89.85 ± 46.70 ng*h*mL^{-1}, $MRT_{0-\infty}$=11.70 ± 4.10 h). In this research, the peak plasma concentration (C_{max}) of glycyrrhizic acid was 528.59 ± 109.52 ng/mL, and its AUC_{0-t} reached 2201.08 ± 1040.42. Peimisine had a longer peak time (T_{max} = 5.37 ± 2.92 h), a lower peak value (C_{max} = 1.59 ± 0.46 ng/mL), and a relatively longer in vivo residence time ($MRT_{0-\infty}$=53.67 ± 42.07 h).

3.4. Network pharmacology

By integrating 13 candidate components selected by chemical profile with 21 components selected by metabolite profile and PK profile, 22 candidate Q-markers were selected. As shown in **Fig. 6A**, an overlap of 46 targets was simultaneously involved in the interactions with 22 Q-marker candidates and the regulation of inflammation, suggesting that these targets formed a network target group (Wang et al., 2022) for the anti-inflammatory effect of JZOL. To reveal the relationship among these targets, the protein–protein interaction (PPI) network was constructed as shown in **Fig. 6B** and sequent subnetwork extraction showed that 12 targets in Mode 1 (BCL2L1, MAPK8, PPARG, MAPK14, HSP90AA1, IKBKB, NOS2, PTGS2, NFKB1, CASP1, GAPDH, TLR9) have had the most significant interaction association and were likely to be the core of the network target group. The further pharmacological network analysis (**Fig. 6C**) also suggests that these targets from a broad
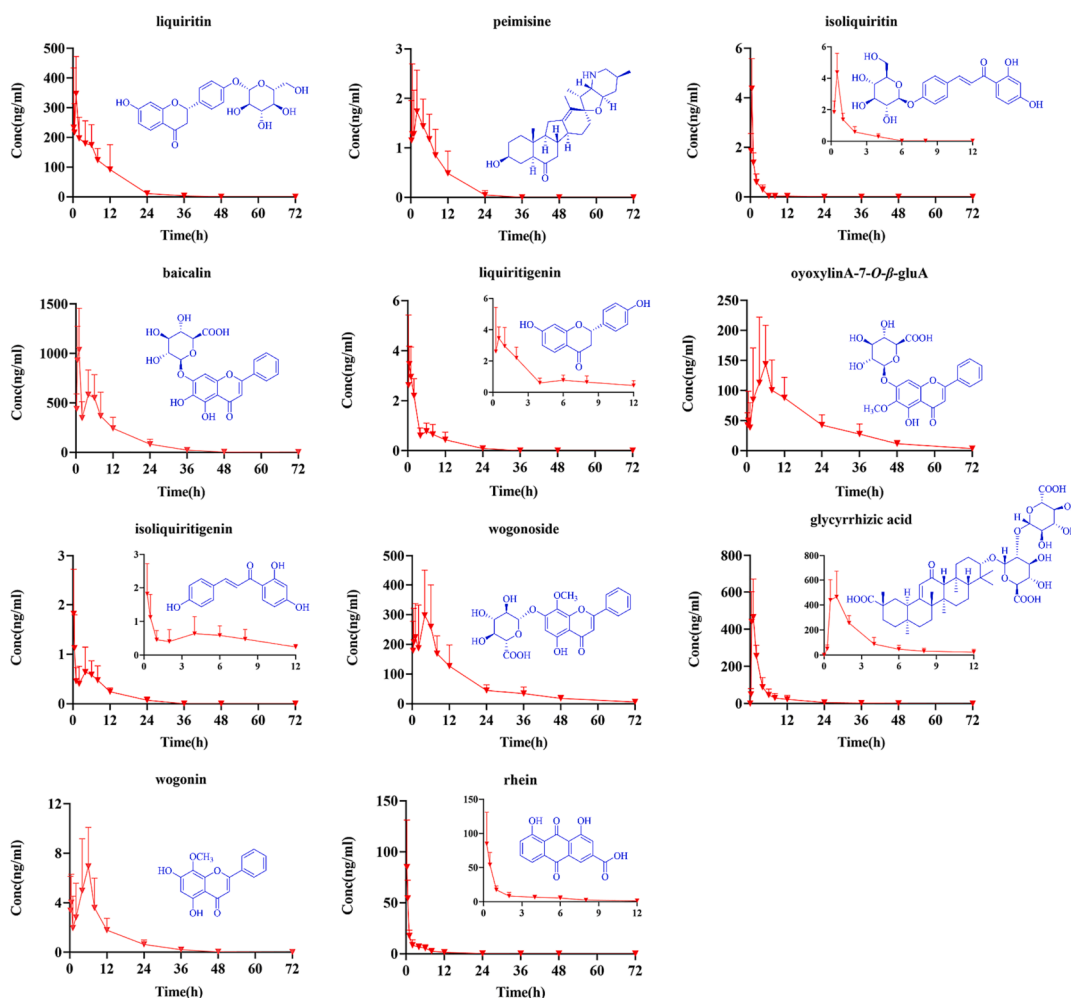
Fig. 5. Comparison of serum concentration–time curves of 11 analytes in JZOL (n = 7).

Table 2
Pharmacokinetic parameters of 11 ingredients from JZOL after oral administration in rats (n = 7).

Name	T_{max} (h)	$t_{1/2}$ (h)	C_{max} (ng/mL)	AUC_{0-t} (ng*h*mL^{-1})	$AUC_{0-\infty}$ (ng*h*mL^{-1})	MRT_{0-t} (h)	$MRT_{0-\infty}$ (h)
liquiritin	2.54 ± 2.44	4.16 ± 1.92	138.02 ± 40.22	1086.90 ± 344.28	1111.93 ± 343.32	6.87 ± 1.88	7.52 ± 1.80
peimisine	5.37 ± 2.92	38.29 ± 32.94	1.59 ± 0.46	18.36 ± 2.28	35.16 ± 16.40	13.62 ± 3.78	53.67 ± 42.07
isoliquiritin	0.50 ± 0.00	1.39 ± 0.27	4.59 ± 1.33	4.72 ± 0.87	4.78 ± 0.87	1.39 ± 0.25	1.51 ± 0.23
baicalin	4.33 ± 0.82	11.15 ± 5.40	1134.15 ± 550.36	9650.72 ± 5013.90	10596.89 ± 5194.60	12.93 ± 3.37	17.47 ± 8.83
liquiritigenin	0.75 ± 0.27	7.28 ± 2.09	4.05 ± 0.75	14.79 ± 3.49	17.27 ± 5.78	5.56 ± 1.14	8.61 ± 2.55
oyoxylinA-7-O-β-D-gluA	9.37 ± 8.11	50.93 ± 35.79	98.97 ± 63.50	2164.23 ± 1398.77	3531.70 ± 2526.75	25.78 ± 5.50	70.06 ± 44.04
wogonoside	5.37 ± 3.86	15.85 ± 7.13	343.88 ± 223.12	3685.52 ± 869.65	4011.55 ± 1089.60	18.02 ± 5.03	23.87 ± 9.00
isoliquiritigenin	0.37 ± 0.14	8.80 ± 6.26	2.01 ± 0.84	8.10 ± 2.02	9.69 ± 3.19	7.69 ± 0.87	12.70 ± 7.13
glycyrrhizic acid	1.92 ± 1.71	9.27 ± 2.60	528.59 ± 109.52	2201.08 ± 1040.42	2323.70 ± 1141.28	5.93 ± 1.66	7.92 ± 3.16
wogonin	7.95 ± 2.54	5.32 ± 0.62	8.73 ± 2.74	72.45 ± 24.00	72.68 ± 24.00	9.91 ± 1.04	10.07 ± 1.04
rhein	0.42 ± 0.13	9.86 ± 2.73	18.98 ± 7.19	87.12 ± 46.50	89.85 ± 46.70	9.38 ± 3.01	11.70 ± 4.10

interaction with all 22 compounds, with targets like PTGS2 and CASP1 potentially playing a more important role by interacting with more compounds than other targets. The further signaling pathway analysis also suggested that "signaling by interleukins" and "cytokine signaling in immune system" were the top two significant pathways (Fig. 6**D**) and were mainly associated with most of the targets in Mode 1 (Fig. S7). As for the regulatory effect of Gypsum Fibrosum and Chloriti Lapi, it's indicated that nine targets (CXCR4, HPSE, LTB4R, PLA2G4A, PRKCA, PRKCQ, PRKCG, PTAFR, TRPV1) among the network target group (Fig. 6**A**) were involved in the interaction with the ionic composition in Gypsum Fibrosum and Chloriti Lapis. All nine targets, except HPSE, were recognized for Gypsum Fibrosum and Chloriti Lapis, probably due

to the common ionic composition of Ca^{2+}. These targets mainly played an auxiliary role by affecting pathways such as "signaling by GPCR" (Fig. S8), which is consistent with the Chinese medicine theory that Gypsum Fibrosum and Chloriti Lapis mainly assist other herbs in exerting their function.

The binding affinities between 46 targets in the network target group and 22 Q-marker candidates of JZOL were evaluated further through molecular docking, as shown in Fig. 7**A**. It can be seen that all compounds, except Glycyrrhizic acid and Licoricesaponin G$_2$, formed a direct interaction with the network target group. These two compounds might exert indirect regulation with the targets related to Gypsum Fibrosum and Chloriti Lapis, as shown in Fig. 6**C**. Based on the cutoff of
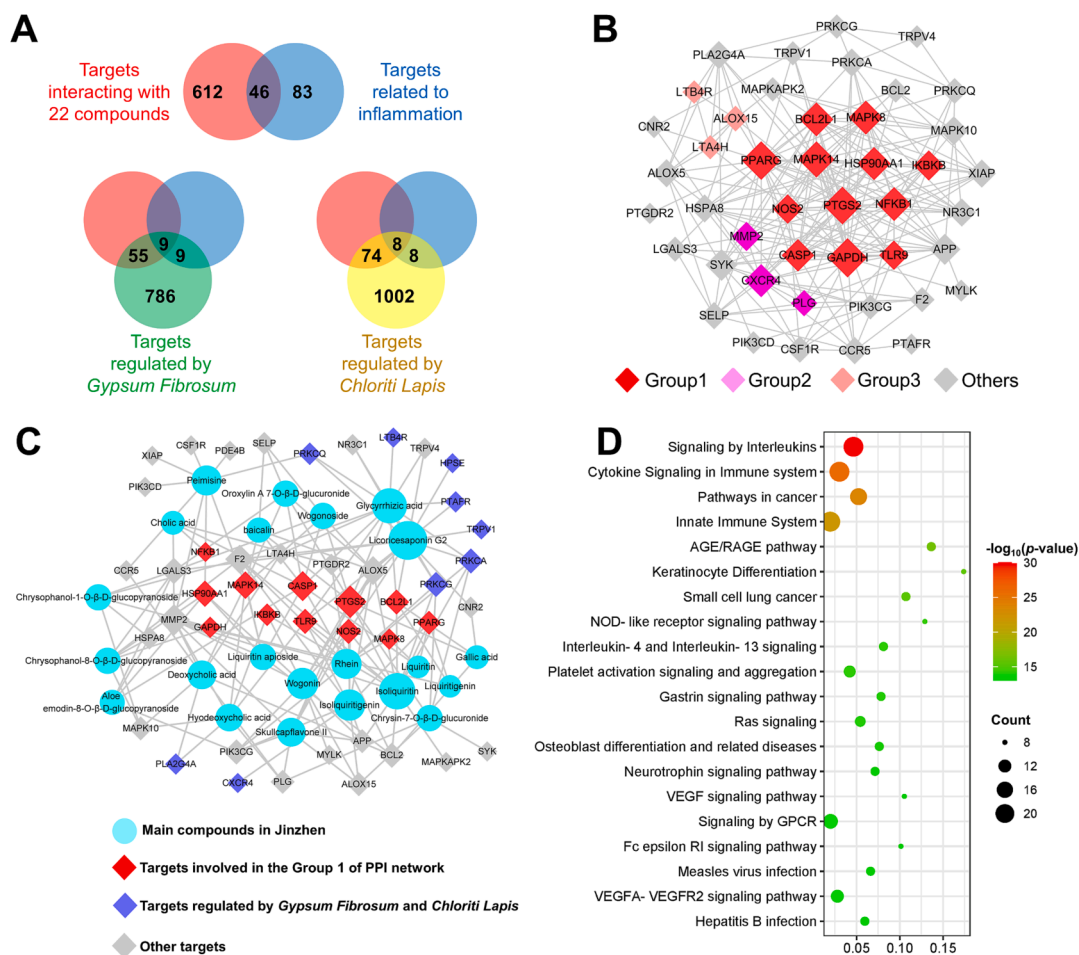
Fig. 6. The potential regulation effect of 22 Q-marker candidates as well as *Gypsum Fibrosum* and *Chloriti Lapis* in JZOL via the network pharmacology analysis. (A) The Venn diagram for the discovery of 46 key targets from different target sets, namely targets interacting with compounds, targets related to inflammation, targets regulated by *G. Fibrosum* and targets regulated by *C. Lapis*. (B) The main target interaction mode recognized by the protein–protein interaction analysis. (C) The pharmacological network involved in the 22 Q-marker candidates in JZOL and ions in *G. Fibrosum* and *C. Lapis*. (D) The top 20 significant signaling pathways by GSEA analysis.

binding affinities, the Q-marker candidates showed different levels of importance in targeting the network target group, as indicated by the statistics of target numbers (Fig. 7**B**).

3.5. Candidate Q-markers prediction based on multi-factor analysis

A table filled with five factors corresponding to 22 selected components was input to the SPSSPRO website for multi-factor analysis. Firstly, through pre-computation and applicability test, the statistic Kaiser-Meyer-Olkin (KMO) values were 0.645, which were greater than 0.6, and the p values of Bartlett's Test were equal to 0.000, reaching a very significant level. This indicates that the 22 candidate Q-markers covering five factors were suitable for factor analysis (**Table S10, S11**). Based on the result of the explanation rate of cumulative variance after rotation, the common factors were determined as three, which explained the information of 97.1 % of the original data (X1 = 56.11 %, X2 = 20.92 %, and X3 = 20.11 %). The three common factors were mainly attributed to C_{max} (PK result), compatibility, and network pharmacology, indicating their importance in distinguishing candidate Q-markers. According to Eq (2)–(3), the F value for each candidate Q-marker was then calculated between −0.70 to 2.87, and component **30** (baicalin, F = 2.87), component **39** (oroxylin A 7-*O*-β-D-glucuronide, F = 0.44), and component **38** (chrysin-7-*O*-β-D-glucuronide, F = 0.41) were the top three ingredients (Table 3). It is worth noting that the F

score for baicalin is almost five times that of the second chemical, preliminarily proving the importance of baicalin in JZOL, as stated in the 2020 edition of the Pharmacopoeia of the People's Republic of China.

Based on the results of the multi-factor analysis, seven components (aloeemodin-8-*O*-β-D-glucopyranoside, baicalin, chrysin-7-*O*-β-D-glucuronide, oroxylin A 7-*O*-β-D-glucuronide, wogonoside, chrysophanol-8-*O*-β-D-glucopyranoside, skullcapflavone II) were selected as candidate Q-markers of JZOL with the F > 0.

3.6. Activity evaluation

The anti-inflammatory activities of the above seven candidate Q-markers were further verified through anti-inflammatory assays, with two chemicals (**16** and **79**) with F < 0 selected as negative controls. Firstly, all chemicals were screened at respective maximum non-toxic concentrations. The concentrations of compounds **13**, **16**, **30**, **38**, **39**, **45**, **46**, **74** and **79** were 50, 100, 50, 3.13, 50, 12.5, 3.13, 12.5, and 3.13 μg/ml, respectively. As shown in Fig. 8, baicalin (**30**), oroxylin A 7-β-D-glucuronide (**39**) and wogonoside (**46**) showed significant anti-inflammatory activities in inhibiting the production of inflammatory factors (NO, IL-6, IL-1β, and PGE₂) in LPS-induced RAW264.7 cells. Compounds **13** and **38** could effectively reduce the release of NO and PGE₂; compound **45** has a significant effect on reducing the release of IL-1β and PGE₂ at a lower concentration range, and compound **74** showed
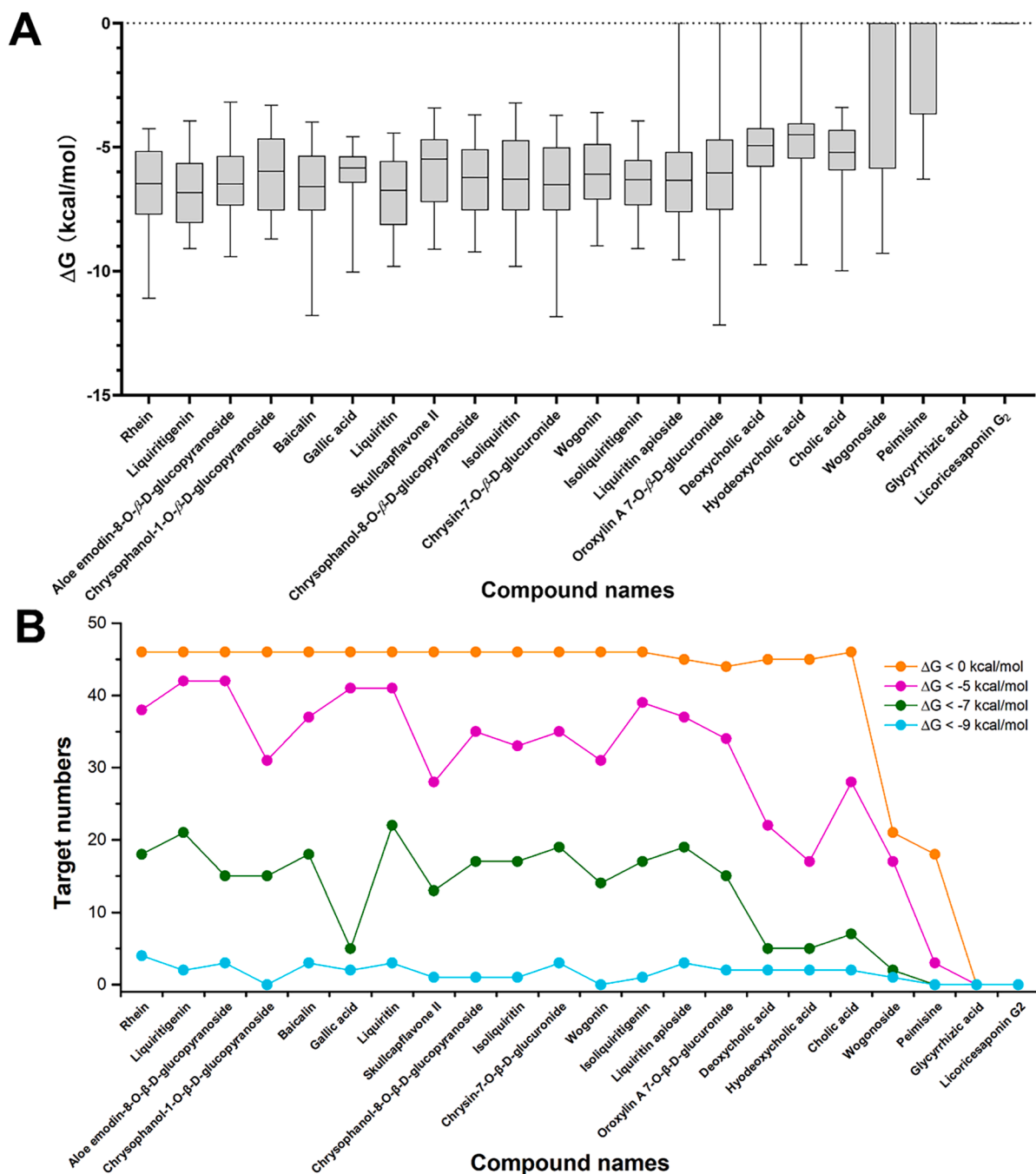
Fig. 7. The affinity evaluation between 22 Q-marker candidates and 46 key targets by molecular docking. (A) The affinity (ΔG) distribution for 22 Q-marker candidates when interacting 46 key targets were evaluated by boxplot. (B) The importance of candidates analyzed by the number of interacting targets with different affinity cutoffs (0, −5, −7, −9 kcal/mol).

substantial reduction in the release of IL-6 and NO. Although compounds **16** and **79** showed no obvious therapeutic effect on the constructed cell model and evaluation indicators in this experiment, it further demonstrated that the rationality of the strategy used in this study in balancing the various properties of the Q-markers simultaneously and in screening out suitable anti-inflammatory Q-markers from hundreds and thousands of ingredients in TCMps.

4. Discussion

The "multi-component, multi-target and multi-pathway" feature of TCMps poses significant challenges in achieving dependable quality

control, which is a crucial factor restricting the modernization process of traditional Chinese medicine (Yang et al., 2017, He et al., 2018). To enhance the quality standards, it is necessary to identify Q-markers that can represent the entire formula and establish scientific methods for evaluation. In this study, we focus on JZOL as an example and delve into the discovery of quality markers for TCMps. JZOL is a Chinese herbal formula used for treating acute bronchitis in children for hundreds of years. According to the "Pharmacopoeia of the People's Republic of China in 2020'', the quality standard for JZOL is to control the content of baicalin not lower than 0.25 mg/ml. However, a single-component standard is insufficient for Chinese herbal formulas due to their multiple components, targets, and mechanisms of action. Currently, research

Table 3
Comprehensive score of candidate Q-markers from JZOL by multi-factors analysis.

Rank	Name	F value	Compatibility (min–max standardized)	System pharmacology (min–max standardized)	Cmax (min–max standardized)	Content (min–max standardized)	AUC0-∞ (min–max standardized)
1	Baicalin	2.87	1.00	0.82	1.00	1.00	1.00
2	Oroxylin A 7-*O*-β-ᴅ-glucuronide	0.46	1.00	0.68	0.09	0.09	0.33
3	Chrysin-7-*O*-β-ᴅ-glucuronide	0.41	1.00	0.86	0.18	0.01	0.19
4	Wogonoside	0.38	1.00	0.09	0.30	0.21	0.38
5	Skullcapflavone II	0.20	1.00	0.59	0.18	0.00	0.19
6	Chrysopyranol-8-*O*-β-ᴅ-glucopyranoside	0.06	0.50	0.77	0.18	0.01	0.19
7	Aloeemodin-8-*O*-β-ᴅ-glucopyranoside	0.02	0.50	0.68	0.18	0.03	0.19
8	Hyodeoxycholic acid	−0.03	0.50	0.23	0.18	0.26	0.19
9	Liquiritin	−0.09	0.00	1.00	0.12	0.12	0.10
10	Wogonin	−0.10	1.00	0.64	0.01	0.00	0.01
11	Cholic acid	−0.10	0.50	0.32	0.18	0.13	0.19
12	Glycyrrhizic	−0.13	0.00	0.00	0.47	0.35	0.22
13	Liquirtin apioside	−0.15	0.00	0.86	0.18	0.00	0.19
14	Gallic acid	−0.18	0.50	0.23	0.18	0.11	0.19
15	Rhein	−0.24	0.50	0.82	0.02	0.00	0.01
16	Deoxycholic acid	−0.30	0.50	0.23	0.18	0.00	0.19
17	Chrysopyranol-1-*O*-β-ᴅ-glucopyranoside	−0.35	0.50	0.68	0.00	0.00	0.00
18	Liquiritigenin	−0.41	0.00	0.95	0.00	0.02	0.00
19	Peimisine	−0.52	1.00	0.00	0.00	0.00	0.00
20	Isoliquiritin	−0.55	0.00	0.77	0.00	0.00	0.00
21	Isoliquiritigenin	−0.55	0.00	0.77	0.00	0.00	0.00
22	Licorice-saponin G2	−0.71	0.00	0.00	0.18	0.00	0.19
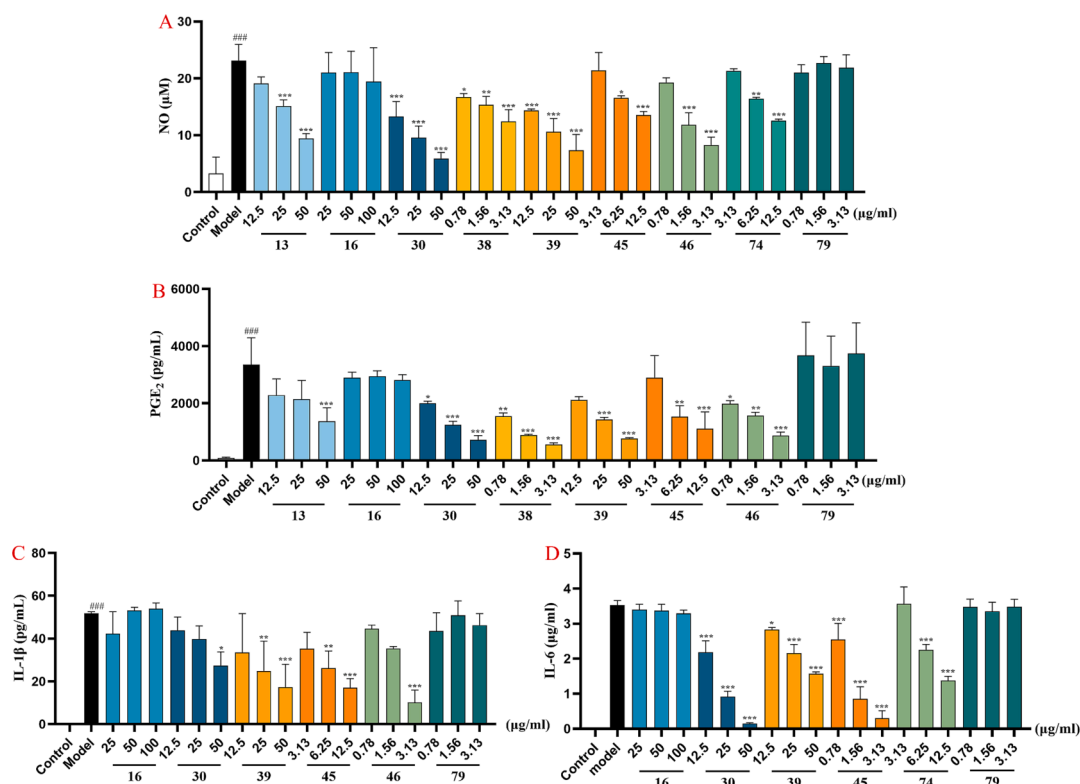
Fig. 8. The anti-inflammatory activity evaluation of compounds **13**, **16**, **30**, **38**, **39**, **45**, **46**, **74** and **79** with the LPS- induced RAW264.7 cell model ($\bar{x} \pm s$, n = 3). (A) statistical analysis of inhibition on NO production, (B) statistical analysis of inhibition on PGE$_2$ production, (C) tatistical analysis of inhibition on IL-1β production, (D) statistical analysis of inhibition on IL-6 production. Cells were exposed to three different administration concentrations (low, medium, high) of compounds and LPS. $^{###}p < 0.001$ vs. control group and $^{***}p < 0.001$, $^{**}p < 0.01$, $^{*}p < 0.05$ vs. LPS-treated group.

on JZOL mainly focuses on the identification of active substances and the exploration of its mechanisms of action, with limited studies on improving quality control standards. Therefore, this study proposes a comprehensive multi-factor analysis strategy by conducting systematic investigations into the chemical composition, pharmacokinetics, and network pharmacology of JZOL. The goal is to screen representative anti-inflammatory quality markers for JZOL and validate their reliability through anti-inflammatory activity evaluation.

In our research, UPLC-Q/TOF-MS enables precise JZOL chemical identification with high resolution and accurate mass measurement, while UPLC-QqQ-MS facilitates pharmacokinetic profile characterization with high sensitivity and selective quantification. However, the animal-derived and mineral drugs were fall to detecte by MS technology. We conducted qualitative and quantitative analysis of the amino acid components in JZOL to elucidate the potential contribution of animal drugs in the formulation in our previous research (Li et al., 2020b). In our current research, network pharmacology was employed to identify key targets related to mineral drugs and their interactions with the screened components, aiming to elucidate the mechanism of action of mineral drugs in JZOL. Furthermore, a novel "multi-factor analysis" strategy was introduced to address the Q-marker screening successfully. The strategy was applied to determine anti-inflammatory Q-markers of JZOL by integrating chemical profile characterization, PK research, and network pharmacology research. Ultimately, seven components were selected as anti-inflammatory Q-markers of JZOL, namely aloeemodin-8-*O*-β-D -glucopyranoside (**13**), baicalin (**30**), chrysin-7-*O*-β- D -glucuronide (**38**), oroxylin A 7-*O*-β- D -glucuronide (**39**), wogonoside (**46**), chrysophanol-8-*O*-β- D -glucopyranoside (**45**), and skullcapflavone II (**74**). The anti-inflammatory activity of the seven Q-markers was further verified to confirm the rationality. Furthermore, the result showed that baicalin was superior to other components in reducing productions of NO, IL-6, IL-1β and PGE$_2$, which consisted with the finding of previous studies that polymethoxy flavones have greater anti-inflammatory activity (Wang et al., 2014). Therefore, baicalin was determined as the most important Q-markers of JZOL, corresponding to the current quantitative indicator of JZOL recorded by "Pharmacopoeia of the People's Republic of China in 2020''.

Although the "multi-factor analysis" strategy represents a promising approach to discovering Q-markers in quality control research of TCMps, the study still have some limitations. Firstly, the selected factors have a greater impact on the screening of Q-markers, and the research results could not screen out the components that exist in animal drugs (Caprae Hircus Cornu). Secondly, the visualization of the method and the obtained results are insufficient. Furthermore, our research mainly focuses on the anti-inflammatory activities, the result presented the anti-inflammatory Q-markers. Other ingredients of JZOL may exert therapeutic effects through other pathways of activation: liquiritin mediated the antitussive effects through dual inhibition of TRPV1 and TRPA1 channels (Liu et al., 2020). And hyodeoxycholic acid may serve efforts in antipyretic of JZOL (Zhang et al., 2016).

5. Conclusion

In this study, a "multi-factor analysis" strategy was conducted to analyze the compatibility contribution of herbal medicines, the content, the *in vivo* PK characteristics, and the degree of network pharmacology of the components, aiming to select suitable anti-inflammatory Q-markers of JZOL. As a result, a total of seven ingredients (aloeemodin-8-*O*-β-D-glucopyranoside, baicalin, chrysin-7-*O*-β-D-glucuronide, oroxylin A 7-*O*-β-D-glucuronide, wogonoside, chrysophanol-8-*O*-β-D-glucopyranoside, and skullcapflavone II) with better anti-inflammatory activity were selected as anti-inflammatory Q-markers of JZOL. This new strategy provides new insights for the discovery of quality markers in TCMps and lays a solid foundation for their quality control improvement.

Declaration of Competing Interest

The authors declare that they have no known competing financial interests or personal relationships that could have appeared to influence the work reported in this paper.

Appendix A. Supplementary material

Supplementary data to this article can be found online at https://doi.org/10.1016/j.arabjc.2023.105433.

References

W.N. Amala R.A.Z. Aziz N. Rohmah H.N. Imtiyaz M.D.I. Iskandar E.R. Purnama In silico Exploration on The Potency of Basil (Ocimum basilicum) as an Anti-Aging Skin Agent Bioactivities. https:// 2023 doi.org/10.47352/bioactivities.2963-654X.193.

Chen, W., Yang, Y., Fu, K., Zhang, D., Wang, Z., 2022. Progress in ICP-MS analysis of minerals and heavy metals in traditional medicine. amage. Front. Pharmacol. 13 https://doi.org/10.3389/fphar.2022.891273.

Chu, Y., Wang, M., Wang, X., Zhang, X., Liu, L., Shi, Y., Zuo, S., Du, S., Kang, J., Li, B., Cheng, W., Sun, Z., Zhang, X., 2022. Identifying quality markers of Mailuoshutong pill against thromboangiitis obliterans based on chinmedomics strategy. Phytomedicine 104, 154313. https://doi.org/10.1016/j.phymed.2022.154313.

Cui, X., Liang, L., Geng, H., Liu, Y., Xi, J., Wang, J., Ching, T., Bee, E., Chai, Y., Wu, S., Jin, D., Xie, Y., 2022. Efficacy, safety and mechanism of Jinzhen oral liquid in the treatment of acute bronchitis in children: A randomized, double-blind, multicenter clinical trial protocol. Front. Pharmacol. 13 https://doi.org/10.3389/fphar.2022.948236.

Gao, M., Lan, J., Zhang, Y., Yu, S., Bao, B., Yao, W., Cao, Y., Shan, M., Cheng, F., Zhang, L., Chen, P., 2022. Discovery of processing-associated Q-marker of carbonized traditional Chinese medicine: An integrated strategy of metabolomics, systems pharmacology and in vivo high-throughput screening model. Phytomedicine 102, 154152. https://doi.org/10.1016/j.phymed.2022.154152.

Gfeller, D., Grosdidier, A., Wirth, M., Daina, A., Michielin, O., Zoete, V., 2014. SwissTargetPrediction: a web server for target prediction of bioactive small molecules. Nucleic Acids Res. 42 (W1), W32–W38. https://doi.org/10.1093/nar/gku293.

He, J., Feng, X., Wang, K., Liu, C., Qiu, F., 2018. Discovery and identification of quality markers of Chinese medicine based on pharmacokinetic analysis. Phytomedicine 44, 182–186. https://doi.org/10.1016/j.phymed.2018.02.008.

Hu, Y., Huang, W., Luo, Y., Xiang, L., Wu, J., Zhang, Y., Zeng, Y., Xu, C., Meng, L., Wang, P., 2021. Assessment of the anti-inflammatory effects of three rhubarb anthraquinones in LPS-Stimulated RAW264. 7 macrophages using a pharmacodynamic model and evaluation of the structure-activity relationships. J. Ethnopharmacol. 273, 114027 https://doi.org/10.1016/j.jep.2021.114027.

Ikarashi, N., Ogiue, N., Toyoda, E., Kon, R., Ishii, M., Toda, T., Aburada, T., Ochiai, W., Sugiyama, K., 2012. Gypsum fibrosum and its major component CaSO4 increase

cutaneous aquaporin-3 expression levels. J. Ethnopharmacol. 139 (2), 409–413. https://doi.org/10.1016/j.jep.2011.11.025.

Kuhn, M., Szklarczyk, D., Pletscher-Frankild, S., Blicher, T.H., Von Mering, C., Jensen, L. J., Bork, P., 2014. STITCH 4: integration of protein-chemical interactions with user data. Nucleic Acids Res. 42 (D1), D401–D407. https://doi.org/10.1093/nar/gkt1207.

Y.S. Kurniawan T. Indriani H. Amrulloh L.C. Adi A.C. Imawan K.T.A. Priyangga E. Yudha The Journey of Natural Products: From Isolation Stage to Drug's Approval in Clinical Trials Bioactivities. https:// 2023 doi.org/10.47352/bioactivities.2963-654X.190.

Li, Y.L., Qin, S.Y., Li, Q., Song, S.J., Xiao, W., Yao, G.D., 2023. Jinzhen Oral Liquid alleviates lipopolysaccharide-induced acute lung injury through modulating TLR4/MyD88/NF-κB pathwa. Phytomedicine 114, 154744. https://doi.org/10.1016/j.phymed.2023.154744.

Li, C., Sun, C., Yang, Y., Ma, N., Wang, Y., Zhang, F., Pei, Y., 2022. A novel strategy by integrating chemical profiling, molecular networking, chemical isolation, and activity evaluation to target isolation of potential anti-ACE2 candidates in Forsythiae Fructus. Phytomedicine 96, 153888. https://doi.org/10.1016/j.phymed.2021.153888.

Li, H., Wang, T., Yang, Q., Liu, L., Ma, S., Cao, L., Wang, Z., Yao, X., Yu, Y., Xiao, W., 2020. Overall quality control of Jinzhen Oral Liquid based on HPLC-UVD-ELSD fingerprint and simultaneous determination of 13 main representative components. Chin. Tradit. Herb Drugs 51 (22), 5737–5747. https://doi.org/10.7501/j.issn.0253-2670.2020.22.010.

Li, H., Wang, Q., Qu, W., Wang, T., Cao, L., Wang, Z., Yang, X., Yu, Y., Xiao, W., 2020. Quality control of Jinzhen oral liquid based on amino acids fingerprint and simultaneous determination of 29 amino acdids. Chin. Tradit. Herb Drugs 51 (23), 5972–5979. https://doi.org/10.7501/j.issn.0253-2670.2020.23.009.

Liu, C., Chen, S., Xiao, X., Zhang, T., Hou, W., Liao, M., 2016. A new concept on quality marker of Chinese materia medica: Quality control for Chinese medicinal products. Chin. Tradit. Herb Drugs 47 (9), 1443–1457. https://doi.org/10.7501/j.issn.0253-2670.2016.09.001.

Liu, C., Cheng, J., Guo, D., Zhang, T., Li, Y., Hou, W., Huang, L., Xu, H., 2017. A new concept on quality marker for quality assessment and process control of Chinese medicines. Chin. Herb Med. 9 (1), 3–13. https://doi.org/10.1016/S1674-6384(17)60070-4.

Liu, Z., Wang, P., Lu, S., Guo, R., Gao, W., Tong, H., Yin, Y., Han, X., Liu, T., Chen, X., Zhu, M., Yang, Z., 2020. Liquiritin, a novel inhibitor of TRPV1 and TRPA1, protects against LPS-induced acute lung injury. Cell Calcium 88, 102198. https://doi.org/10.1016/j.ceca.2020.102198.

Liu, C., Xia, T., Luo, Z., Wu, Y., Hu, Y., Chen, F., Tang, Q., Tan, X., 2021. Network pharmacology and pharmacokinetics integrated strategy to investigate the pharmacological mechanism of Xianglian pill on ulcerative colitis. Phytomedicine 82, 153458. https://doi.org/10.1016/j.phymed.2020.153458.

Liu, J., Zhang, G., Huang, G., Li, L., Li, C., Wang, M., Liang, X., Xie, D., Yang, C., Li, Y., 2014. Therapeutic effect of Jinzhen oral liquid for hand foot and mouth disease: a randomized, multi-center, double-blind, placebo-controlled trial. PLoS One 9 (4), e94466.

Lu, Q., Bao, Y., Wang, W., Xie, X., Yu, J., 2010. A prospective multicenter randomized controlled study on the efficacy and safety of Jin-Zhen oral solution. Chin. J. Pract. Pediatrics 25 (5), 383–387.

Ouyang, Y., Tang, L., Hu, S., Tian, G., Dong, C., Lai, H., Wang, H., Zhao, J., Wu, H., Zhang, F., Yang, H., 2022. Shengmai San-derived Compound Prescriptions: a review on Chemical constituents, Pharmacokinetic studies, Quality control, and Pharmacological properties. Phytomedicine 107, 154433. https://doi.org/10.1016/j.phymed.2022.154433.

Schreiber, J., 2021. Issues and recommendations for exploratory factor analysis and principal component analysis. Res. Soc. Admin. Pharm. 17 (5), 1004–1011. https://doi.org/10.1016/j.sapharm.2020.07.027.

Shu, Y., Niu, X., Wu, J., 2018. Clinical effect of Jinzhen oral liquid on bronchitis in children. Guizhou Med. J. 42 (1), 48–50. https://doi.org/10.3969/j.issn.1000-744X.2018.01.018.

Sun, H., Liu, G., Gao, Y., Gao, H., Wang, Y., 2016. Jinzhen oral liquid in the treatment of 43 children with acute bronchitis. Chin. Tradit. Herb Drugs 29 (5), 12–14. https://doi.org/10.3969/j.issn.1001-6910.2016.05.06.

Szklarczyk, D., Gable, A., Nastou, K., Lyon, D., Kirsch, R., Pyysalo, S., Doncheva, N., Legeay, M., Fang, T., Bork, P., Jensen, L., Mering, C., 2021. The STRING database in 2021: customizable protein-protein networks, and functional characterization of user-uploaded gene/measurement sets. Nucleic Acids Res. 49 (18), 10800. https://doi.org/10.1093/nar/gkaa1074.

The Pharmacopoea Commission of PRC, 2020. The Pharmacopoeia of the People's Republic of China, part 1. China Medical Science and Technology Press, Beijing, p. 1164-1165.

Wang, S., Chen, P., Jiang, W., Wu, L., Chen, L., Fan, X., Wang, Y., Cheng, Y., 2014. Identification of the effective constituents for anti-inflammatory activity of Ju-Zhi-Jiang-Tang, an ancient traditional Chinese medicine formula. J. Chromato. A 1348, 105–124. https://doi.org/10.1016/j.chroma.2014.04.084.

Wang, Z., Guo, Y., Li, G., 2016. Current status of standardization of traditional Chinese medicine in China. Evid. Based Complement Altern. Med. 2016, 9123103. https://doi.org/10.1155/2016/9123103.

Wang, Z.Y., Wang, X., Zhang, D.Y., Hu, Y.J., Li, S., 2022. Traditional Chinese medicine network pharmacology: development in new era under guidance of network pharmacology evaluation method guidance. China J. Chin. Mater. Med. 47 (1), 7–17. https://doi.org/10.19540/j.cnki.cjcmm.20210914.702.

Wishart, D., Feunang, Y., Guo, A., Lo, E., Marcu, A., Grant, J., Sajed, T., Johnson, D., Li, C., Sayeeda, Z., Assempour, N., Iynkkaran, I., Liu, Y., Maciejewski, A., Gale, N., Wilson, A., Chin, L., Cummings, R., Le, D., Pon, A., Knox, C., Wilson, M., 2018. DrugBank 5.0: a major update to the DrugBank database for 2018. Nucleic Acids Res. 46 (D1), D1074–D1082. https://doi.org/10.1093/nar/gkx1037.

Xiong, H., Zhang, A., Zhao, Q., Zhao, Q., Yan, G., Sun, H., Wang, X., 2020. Discovery of quality-marker ingredients of Panax quinquefolius driven by high-throughput chinmedomics approach. Phytomedicine 74, 152928. https://doi.org/10.1016/j.phymed.2019.152928.

Yang, Z.H., Wang, B., Ma, Q., Wang, L., Lin, Y.X., Yan, H.F., Fan, Z.X., Chen, H.J., Ge, Z., Zhu, F., Wang, H.,J., Zhang, B.N., Sun, H.D., Feng, L.M., 2021. Corrigendum: potential Mechanisms of Action of Chinese Patent Medicines for COVID-19: a Review. Front. Pharmacol. 12, 770125. https://doi.org/10.3389/fphar.2021.668407.

Yang, W., Zhang, Y., Wu, W., Huang, L., Guo, D., Liu, C., 2017. Approaches to establish Q-markers for the quality standards of traditional Chinese medicines. Acta Pharm. Sin. B 7 (4), 439–446. https://doi.org/10.1016/j.apsb.2017.04.012.

Zhang, Y., Gu, B., 2016. Jinzhen oral liquid in the treatment of 50 cases of acute bronchitis. World Latest Med. Inform. 16 (60), 156–163. https://doi.org/10.3969/j.issn.1671-3141.2016.60.118.

Zhang, J., Li, H., Liu, L., Shi, D., Wang, Z., Cao, L., Yao, X., Xiao, W., Yu, Y., 2022. Characterization the xenobiotics of Jinzhen Oral Liquid in rats based on UPLC-Q/TOF-MS. Chin. Tradit. Herb Drugs 53 (10), 2956–2967. https://doi.org/10.7501/j.issn.0253-2670.2022.10.004.

Zhang, Z., Qin, L., Peng, L., Zhang, Q., Wang, Q., Lu, Z., Song, Y., Gao, X., 2016. Pharmacokinetic-pharmacodynamic modeling to study the antipyretic effect of Qingkailing injection on pyrexia model rats. Molecules 21 (3), 317. https://doi.org/10.3390/molecules21030317.

Zhu, X., An, W., Li, X., Zhou, B., Li, H., 2023. Anti-inflammatory effects of Scutellaria baicalensis water extract in LPS-induced THP-1 Macrophages through metabolomics study. Ara. J. Chem. 16 (3), 104507 https://doi.org/10.1016/j.arabjc.2022.104507.